Joint Observation and Transmission Scheduling in Agile Satellite Networks

Lijun He, Ben Liang, *Fellow, IEEE*, Jiandong Li, *Fellow, IEEE*,
and Min Sheng, *Senior Member, IEEE*

Abstract—Compared with traditional observation satellites, agile earth observation satellites are capable of prolonging observation time windows (OTWs) for targets, which significantly alleviates observation conflicts, thereby facilitating imaging data collection. However, it also leads to more uncertainties in determining the start time to image targets within these longer OTWs for an agile satellite network (ASN) to collect imaging data. Furthermore, these collected data are offloaded only within short transmission time windows between data collectors and data sinks, thus resulting in a transmission scheduling problem. Toward this end, this paper investigates joint observation and transmission scheduling in ASNs, aiming at accommodating more imaging data to be collected and offloaded successfully. Specifically, we formulate the studied problem as integer linear programming (ILP) to maximize the weighted sum of scheduled imaging tasks. Then, we explore the hidden structure of this ILP and transform it into a special framework, which can be solved efficiently through semidefinite relaxation (SDR). To reduce computation complexity, we further propose a fast yet efficient algorithm by combining the advantages of the devised SDR method and a genetic algorithm with special population initialization. Finally, simulation results demonstrate that the proposed algorithm can significantly increase the weighted sum of scheduled tasks.

Index Terms—Agile earth observation satellites, time windows, observation scheduling, transmission scheduling.

1 Introduction

As an important space information acquisition platform, the earth observing network (EON) leverages earth observation satellites (EOSs) located in polar orbits to continuously supply earth observation data. The EON has been integrated within diversity space applications such as meteorology, environmental monitoring, and natural disaster surveillance [1]. However, the fast proliferation of these space applications has brought a tremendous increase in demand for the collection of earth observation data. Toward this end, by enhancing the maneuverability of EOSs, the advent of agile satellite networks (ASNs) contributes to alleviate this issue. Specifically, non-agile EOSs can roll themselves to take pictures only when flying over targets. In comparison, as shown in Fig. 1, agile earth observation satellites (AEOSs) in ASNs not only can roll but also pitch themselves agilely to image before or after flying over targets. As a result, the agility of AEOS extends each starting imaging time point to a time interval, termed as the observation time window (OTW). That is, an AEOS can start to image a target at any time within these OTWs, which significantly alleviates observation conflicts, thereby facilitating observation data collection [2].

At the same time, this agility also results in more uncertainties in observation resource allocation for ASNs. Particularly, one needs to determine the start time of imaging a target within multiple OTWs instead of fixed time points. It is therefore essential to effectively allocate observation resources within multiple OTWs for ASNs, aiming at reducing observation conflicts, such that earth observation data can be collected as efficiently as possible.

Furthermore, the phenomenal growth of earth observation data results in more collected data to offload from diverse space information acquisition platforms to data sinks, e.g., ground stations (GSs) [3]. However, the transmission resource of the current systems is insufficient to support these collected data, despite operating in the super high frequency or extremely high frequency bands. The reasons mainly come from three aspects: 1) The amount of imaging data grows fast. As the National Aeronautics and Space Administration (NASA) of the United States projected, the size of pure climate data could grow up to 350 petabytes by 2030 [4]. This phenomenon is exacerbated especially in ASNs, due to the fact that the enhanced maneuverability of EOSs results in a larger amount of observation data to offload. 2) The high-speed movement of AEOSs leads to very limited intermittent contact time. More specifically, the data collectors can offload their collected data only when flying within the coverage of data sinks. That is, the data offloading operations occur only in contact time windows, termed as transmission time windows (TTWs). However, the size of TTWs is in general very small, e.g., a satellite located in polar orbits accesses a GS for only 10 minutes at a time [5]. 3) The terrestrial deployment of GSs is affected by a number of integrated factors, such as national boundaries and politics. It is therefore difficult to achieve global large-scale deployment of GSs. In view of these challenges, it is imperative to jointly consider the ob-

This work was supported in part by the Natural Science Foundation of China under Grant U19B2025, Grant 61725103, and Grant 62001347, in part by the China Postdoctoral Science Foundation under Grant 2019TQ0241 and Grant 2020M673344, in part by Natural Science Basic Research Program of Shaanxi Province under Grants 2021JQ126, and in part by the National Natural Science Foundation of China under Grant 61901388. (Corresponding author: Jiandong Li.)

Lijun He, Jiandong Li, and Min Sheng are with the State Key Laboratory of Integrated Service Networks, Xidian University, Xi'an, Shaanxi, 710071, China (e-mail: lijunhe@stu.xidian.edu.cn; {jdli,msheng}@mail.xidian.edu.cn). Ben Liang is with the Department of Electrical and Computer Engineering, University of Toronto, Toronto, Canada (e-mail: liang@ece.utoronto.ca).

servation resource allocation problem with the allocation of transmission resources, to accommodate more observation data to be collected and offloaded successfully.

Several new challenges arise in addressing this multi-resource allocation problem in ASNs for the following reasons: Firstly, compared with non-agile EOSs, the maneuverability of AEOSs for image acquisitions broadens the starting imaging time from fixed time points to OTWs, thereby generating a considerably larger solution space. Secondly, the enhanced observation abilities of AEOSs contribute to the completion of more scheduled observation tasks, such that a larger amount of imaging data needs to be offloaded. Last but not least, several complicated dependent constraints in both time and space domains exist in ASNs, which exacerbates a wide range of resource conflicts. Hence, our main problem is how to characterize these complicated dependent constraints and resolve various resource conflicts in ASNs, with the aim of achieving efficient imaging data collection and transmission.

To address the aforementioned challenges, we jointly optimize the observation and transmission resources within various time windows for ASNs, aiming to address a weighted sum maximization problem, constrained by complicated dependent constraints in space and time domains. The main contributions of our work are summarized in the following:

- We put forward a joint optimization framework with the consideration of observation and transmission resource allocation together to maximize the weighted sum of scheduled tasks in ASNs. In particular, our proposed framework incorporates various time windows and the complicated dependent constraints in time and space domains from realistic scenarios, thereby charactering the features of real ASNs.
- We explore the underlying structure of a weighted sum maximization problem and transform it into a special integer linear programming (ILP) problem, which can be efficiently handled by utilizing semidefinite relaxation (SDR). Next, we reformulate the resulting ILP as a quadratically constrained quadratic programming problem (QCQP), followed by converting it into the standard form of SDR. Thereafter, in Section 4.1, we give a preliminary design by utilizing SDR to solve the studied problem directly.
- We further propose a hierarchical solution termed Joint Observation and Transmission Scheduling Algorithm with Agile Satellites (JOTSAS), which utilizes the above SDR design but has dramatic reduction in computation cost. Specifically, we first replace three-dimensional variables by two-dimensional variables, and then equivalently decompose the weighted sum maximization problem into a high-level master problem (i.e., the hybrid time window association problem) and a low-level subproblem (i.e., the time window resource allocation problem). We show that simple modifications to the preliminary SDR-based method can solve the low-level subproblem efficiently over its smaller search space, thereby enabling a quick response to the master problem, i.e., the weighted sum of successfully scheduled tasks. We then adopt a genetic framework to solve the master problem, proposing a novel conflict-driven population initialization method (CPInit), to update the time window association strategies to maximize the utility of ASNs.
- Extensive simulations on ASNs demonstrate the following results: 1) Our proposed algorithm outperforms the alternatives in terms of the weighted sum of scheduled tasks. 2) The efficient joint scheduling of observation and transmission leads to substantially higher performance of ASNs.

The remainder of this paper is outlined as follows. In Section 2, we provide an overview of the related work. Section 3 presents the system model and the problem formulation. Section 4 elaborates the proposed algorithms to solve the studied problem. In Section 5, we present simulation results and discussions. Finally, we give concluding remarks in Section 6.

2 Related Work

In this section, we first discuss observation resource allocation in ASNs and then transmission resource allocation in non-agile EOSs. Subsequently, we introduce the joint observation and transmission resource allocation in non-agile EOSs. Finally, we detail the resource allocation in a similar scenario, i.e., the sensor network.

2.1 Observation Resource Allocation in ASNs

There are many existing studies on the resource allocation problem for ASNs to schedule their observation tasks. In particular, the authors of [6] surveyed current literature on the problem of observation resource scheduling. We classify these works into two categories. In the first category, the authors focused on a single agile satellite and devised metaheuristic algorithms (e.g., local search [7], hybrid differential evolution [8], neighborhood search [9]) and machine learning [10]. In the second category, the authors considered multiple agile satellites. Specifically, [11] extended the neighborhood search method in [9] to the scenario of multiple agile satellites. In [12], a real-time task scheduling scheme was proposed to respond to unexpected environmental changes in multiple agile satellite networks. The authors of [13] addressed task scheduling with multiple observations aiming at maximizing the entire observation profit, which is nonlinear in the number of observations. In [14], the authors considered a many-objective agile satellite mission planning problem. In [15], the authors proposed a generic Markov decision process model based on reinforcement learning aiming to solve the agile satellite scheduling problem. The authors of [16] investigated the satellite scheduling problem with consideration for the impact of clouds. However, the above works focus only on observation resource allocation without taking into account the scheduling of transmission resources.

2.2 Transmission Resource Allocation in Non-Agile EOSs

It is imperative to address the scheduling of transmission resources aiming at efficiently offloading the collected data

within the short contact time windows. In [17], a collaborative data downloading algorithm was developed by jointly scheduling inter-satellite links and satellite-ground links. The authors of [18] raised a two-phase task scheduling scheme to dynamically schedule the GEO-LEO communication links in data relay satellite networks. The authors of [19] devised a scheduling scheme to efficiently allocate transmission resources in space networks by jointly considering data compression and transmission. These works made the assumption that the desired observation data has been collected and stored into the satellites, thereby neglecting observation resource allocation. However, the data collection and transmission procedures incur complicated time-dependent constraints in practical satellite networks, thus greatly limiting the applications of these existing schemes.

2.3 Joint Observation and Transmission Resource Allocation in Non-Agile EOSs

By integrating the two phases of data observation and transmission, some existing works start to focus on the multi-resource allocation problem in non-agile EOSs. The authors of [20] developed a two-phase genetic annealing algorithm to solve the integrated imaging and data transmission scheduling problem under the assumption that the transmission resource is sufficient. In [21], the authors simplified the coupling between download scheduling and mission scheduling to obtain a two-step binary linear programming formulation. Inspired by [17], [22] utilized a transmission time sharing method in the data transmission phase to enable the transmission time sharing among multiple EOSs aiming at the efficient utilization of transmission resources. In [23], an exact branch and price algorithm was devised for the problem of imaging and downloading integrated scheduling by making the assumption that the number of transmission opportunities is significantly less than that of observation opportunities. The authors of [24] formulated a joint scheduling problem that considers weather uncertainties into a mixed integer linear programming model and used a commercial solver to solve it.

However, it is not obvious how to extend the above solutions to the more complicated ASNs, due to their much larger number of degrees of freedom [25]. To the best of our knowledge, there are scarce works to address the joint observation and transmission resource allocation issue in ASNs. In [26], the authors addressed the scheduling problem of agile satellites with download considerations by constructing a simple model, where only three different pitching angles were considered. Furthermore, they excluded the overlaps between OTWs and TTWs, which are often present in practical ASNs, as shown in Fig. 2.

2.4 Resource Allocation in Sensor Networks

Interestingly, we observe that resource allocation with mobile sinks in the context of sensor networks are similar to our studied problem. Specifically, the deployment of mobile data sinks in sensor networks enables data collection from sensor nodes via a single-hop communication link [27]. In line with the pattern of sink mobility, we may broadly categorize these proposed schemes into three categories: random mobility [28], predictable mobility [29], and controlled

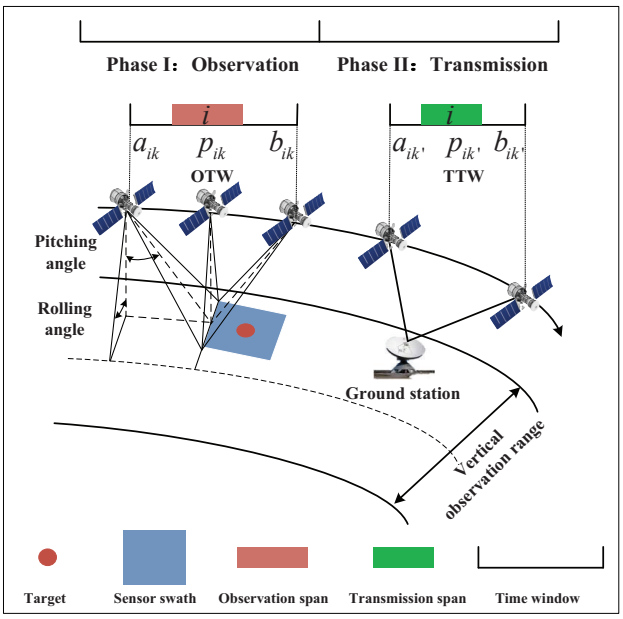

Fig. 1. System scenario.

mobility [30]. The latter two categories specify the mobility path of data sinks, which is similar to the fact that AEOSs circle the earth with their individual orbits. To be specific, in [29], by predicting the mobility path of data sinks, sensor nodes are capable of scheduling sleep and listen periods, thereby optimizing their energy consumption. In [30], a data sink moves along some specified path, which can be stopped or slowed down to maximize communication with sensor nodes. Furthermore, [31] studied a scenario where a data sink (e.g., a LEO satellite) visits the specified area periodically to gather data from deployed sensor nodes. However, none of [29]–[31] can be directly applied to solve our studied problem due to the following reasons: 1) In ASNs, the motion of AEOSs is difficult to control, e.g., stop or slow down; 2) The high-speed and periodic motion of satellite nodes generates a large number of regular contact opportunities, which requires new analytical methods; and 3) In addition to offloading data from data collectors or sensors to data sinks, in this work we are concerned about also the observation resource scheduling of the satellites to collect information.

3 System Model and Problem Formulation

In this section, we first introduce the considered system model and then describe the constraints. Finally, we formulate the problem of maximizing the weighted sum of scheduled tasks.

3.1 System Model

As shown in Fig. 1, we consider an ASN consisting of S AEOSs, denoted by $\mathcal{S} = \{1, ..., S\}$. Each AEOS $s \in \mathcal{S}$ collects the observation data by agilely rolling and pitching to image a set of targets, denoted by $\mathcal{I} = \{1, ..., I\}$. After that, the AEOSs need to transmit the collected imaging data by accessing the data receiver antennas of a set of data sinks, denoted by $\mathcal{H} = \{1, ..., H\}$. In the data observation phase,

(a) Scenario. (b) Overlaps between TTWs and OTWs.

Fig. 2. Illustration of overlaps between TTWs and OTWs , for one observation satellite, three GSs, and ten targets. (a) The simulation scenario. (b) The TTWs and OTWs obtained via the satellite tool kit. It can be seen that the TTWs and OTWs frequently overlap.

AEOS s can image a target $i \in \mathcal{I}$ at any moment within an OTW due to its agility. This means that any moment within an OTW corresponds to an image angle [9]. In addition, the periodic motion of AEOS s generates multiple OTWs associated with target i, denoted by $\mathcal{O}_{i,s}$. Accordingly, we use $\mathcal{O}_{i,\mathcal{S}}$ to indicate the set of OTWs between target i and the S AEOSs. In the data transmission phase, data transmission occurs only when AEOS s flies within the coverage of a data receiver antenna $h \in \mathcal{H}$. That is, AEOS s transmits the collected data only within a TTW. Similarly, the periodicity of AEOS s also produces multiple TTWs associated with antenna h, denoted by $\mathcal{T}_{s,h}$. Moreover, we denote $\mathcal{T}_{\mathcal{S},h}$ as the set of TTWs between the S AEOSs and antenna h. Also, let $\mathcal{T}_{s,\mathcal{H}}$ be the set of TTWs between AEOS s and the H antennas. Accordingly, the notation $\mathcal{T}_{\mathcal{S},\mathcal{H}}$ represents the set of TTWs between S AEOSs and H antennas.

Note that this paper mainly focuses on devising a strategy to jointly allocate the observation and transmission resources in ASNs to efficiently download observation data under some given network resource. As such, we do not consider strategies to increase the amount of data transmission by changing network resource, such as increasing the link bandwidth and optimizing the locations of GSs. In addition, we assume that the data transmission in the second phase is error-free. That is to say, transmission errors in the physical layer can be detected and corrected efficiently by upper-layer protocols. In practical applications, we note that image quality is impacted by different imaging angles. Specifically, a larger imaging angle could lead to a smaller resolution and larger size of the image. In this work, for analytical tractability, we omit the impact of imaging angle on image quality.

3.1.1 Time Window Model

We observe that the OTWs and TTWs represent the time windows, during which AEOSs can conduct the observation and transmission operations, respectively. It is therefore imperative to model these various time windows aiming at characterizing the intermittent connectivity of ASNs. For simplicity, we adopt a two-tuple (a_{ik}, b_{ik}) to indicate time window k associated with target i, where a_{ik} and b_{ik} represent the associated start time and end time, respectively. That is, for an OTW k with respect to AEOS s (e.g., $k \in \mathcal{O}_{i,s}$), the time for AEOS s to execute observation operations should be neither earlier than a_{ik} nor later than b_{ik}. Furthermore, for a TTW k with respect to AEOS s (e.g., $k \in \mathcal{T}_{s,h}$), this means that target i was visible to AEOS s and its imaging data can be downloaded from AEOS s to antenna h within a_{ik} and b_{ik}.

3.1.2 Task Model

We define task i as the process incorporating both the imaging data acquisition and transmission of target i. Also, we consider each task i is associated with a weighted value of w_i. Furthermore, we let p_{ik} denote the processing time of task i within time window k. Particularly, for $k \in \mathcal{O}_{i,s}$, p_{ik} represents the imaging time for AEOS s on image target i, i.e., $p_{ik} = \frac{D_i}{R^{\text{ob}}_{ik}}$, where D_i denotes the amount of imaging data and R^{ob}_{ik} denotes the data collecting rate within OTW k of target i; for $k \in \mathcal{T}_{s,h}$, p_{ik} indicates the transmission time for AEOS s to transmit the imaging data of target i on antenna h, i.e., $p_{ik} = \frac{D_i}{R^{\text{tr}}_{ik}}$, where R^{tr}_{ik} indicates the data transmission rate within TTW k of target i. Moreover, let d_i denote the deadline of task i. Accordingly, we can utilize d_i to update time windows, thus obtaining effective OTWs and TTWs, denoted by $\mathcal{O}^e_{i,s}$, $\mathcal{O}^e_{i,\mathcal{S}}$, $\mathcal{T}^e_{\mathcal{S},h}$, $\mathcal{T}^e_{s,\mathcal{H}}$, and $\mathcal{T}^e_{\mathcal{S},\mathcal{H}}$. More specifically, we replace b_{ik} by d_i if the deadline of task i is within time window k, (i.e., $a_{ik} < d_i < b_{ik}$). Also, we remove time window k if the start time of time window k is larger than the deadline of task i (i.e., $a_{ik} \geq d_i$).

3.2 Constraints

3.2.1 Decision Variable Constraints

To simplify our problem formulation, we first divide the scheduling time horizon into T intervals equally, each indexed by $t \in \mathcal{T} = \{1, ..., T\}$. Each interval is termed as a slot. As shown below, such discretization of the time line is to develop an ILP model, instead of the mixed-integer nonlinear programming model that would result from using a continuous time line. Then, we introduce decision variables $x_{itk} \in \{0, 1\}$ to depict resource assignment including observation and transmission resources. Specifically, if $k \in \mathcal{O}^e_{i,s}$, $x_{itk} = 1$ reveals that AEOS s performs the imaging of target i at time t within OTW k; otherwise $x_{itk} = 0$.

When $k \in \mathcal{T}^e_{s,h}$, $x_{itk} = 1$ indicates that AEOS s transmits the imaging data of target i to antenna h at time t within TTW k; otherwise $x_{itk} = 0$. Each task should be observed and transmitted at most once. This is expressed by the following constraints:

$$\text{C1:} \sum_{\substack{t\in\mathcal{T}\\ k\in\mathcal{O}^e_{i,\mathcal{S}}}} x_{itk} \le 1, \forall i, \qquad \text{C2:} \sum_{\substack{t\in\mathcal{T}\\ k\in\mathcal{T}^e_{\mathcal{S},\mathcal{H}}}} x_{itk} \le 1, \forall i.$$

3.2.2 Sequential Dependency Constraints

In the following, for clarity, we first explain the resource conflicts in ASNs and then introduce constraints that aim to avoid these conflicts.

For any target, an AEOS needs to adjust its attitude to point at it, so it is unable to image two or more targets simultaneously. That is to say, imaging operations for various targets on the same AEOS should be sequential. Here, to indicate this sequential dependency, we introduce binary variables $\lambda_{ijs} \in \{0, 1\}$, so that $\lambda_{ijs} = 1$ indicates that AEOS s first images target i and then target j; otherwise $\lambda_{ijs} = 0$. Let r^{oo}_{ijs} be the time to adjust the attitude of AEOS s such that its sensor points away from target i and points at target j. Then, the following constraints should be met:

$$\text{C3:} \sum_{\substack{t\in\mathcal{T}\\ k\in\mathcal{O}^e_{i,s}}} x_{itk} t \ge \sum_{\substack{t\in\mathcal{T}\\ k\in\mathcal{O}^e_{j,s}}} x_{jtk}(t + p_{jk} + r^{\text{oo}}_{ijs}) - V\lambda_{ijs}, \forall i \ne j, s,$$

$$\text{C4:} \ \lambda_{ijs} + \lambda_{jis} = 1, \forall i \ne j, s,$$

where V is a sufficiently large positive constant.

Furthermore, we assume that each AEOS is equipped with only one transmission antenna to access data receiver antennas. That is, the data transmission time of different tasks cannot overlap each other for the same AEOS. Therefore, we introduce binary variables $\psi_{ijs} \in \{0, 1\}$ to reveal the sequential dependency of various transmission operations conducted by an AEOS, so that $\psi_{ijs} = 1$ indicates that AEOS s first transmits the observation data of target i and then that of target j; otherwise $\psi_{ijs} = 0$. We denote r^{tt}_{ijs} as the time to adjust the attitude of AEOS s such that its transmitting antenna points away from task i and points at task j. Thus, we can obtain the following constraints:

$$\text{C5:} \sum_{\substack{t\in\mathcal{T}\\ k\in\mathcal{T}^e_{s,\mathcal{H}}}} x_{itk} t \ge \sum_{\substack{t\in\mathcal{T}\\ k\in\mathcal{T}^e_{s,\mathcal{H}}}} x_{jtk}(t + p_{jk} + r^{\text{tt}}_{ijs}) - V\psi_{ijs}, \forall i \ne j, s,$$

$$\text{C6:} \ \psi_{ijs} + \psi_{jis} = 1, \forall i \ne j, s.$$

For data transmission, we assume that each data receiver antenna can only accommodate one AEOS. Accordingly, we use binary variables $\gamma_{ijh} \in \{0, 1\}$ to represent the sequence of transmission operations for the same antenna. In particular, $\gamma_{ijh} = 1$ means that the data transmission of target i is before that of target j on antenna h; otherwise $\gamma_{ijh} = 0$. Let l_{ijh} denote the rotation time of data receiver antenna h from pointing at task i to pointing at task j. To avoid the transmission data block of different targets overlapping each other on the same antenna, we require the following constraints:

$$\text{C7:} \sum_{\substack{t\in\mathcal{T}\\ k\in\mathcal{T}^e_{\mathcal{S},h}}} x_{itk} t \ge \sum_{\substack{t\in\mathcal{T}\\ k\in\mathcal{T}^e_{\mathcal{S},h}}} x_{jtk}(t + p_{jk} + l_{ijh}) - V\gamma_{ijh}, \forall i \ne j, h,$$

$$\text{C8:} \ \gamma_{ijh} + \gamma_{jih} = 1, \forall i \ne j, h.$$

We assume that an AEOS cannot image a target and transmit captured data at the same time. From the perspective of practical applications, this assumption is reasonable because the probability that an AEOS can simultaneously observe and transmit is extremely low in practical systems due to the strict requirements of satellite attitudes toward either an imaging target or a data receiver antenna. Here, binary variables $\theta_{ijs} \in \{0, 1\}$ are utilized to reveal the sequential dependency of observation and transmission operations on the same AEOS. Specifically, $\theta_{ijs} = 1$ represents the following two cases for AEOS s: either it first images task i and then transmits the data for task j, or it first images task j and then transmits the data for task i. Hence, we have the following constraints:

$$\text{C9:} \sum_{\substack{t\in\mathcal{T}\\ k\in\mathcal{O}^e_{i,s}}} x_{itk} t \ge \sum_{\substack{t\in\mathcal{T}\\ k\in\mathcal{T}^e_{s,\mathcal{H}}}} x_{jtk}(t + p_{jk} + r^{\text{ot}}_{ijs}) - V\theta_{ijs}, \forall i \ne j, s,$$

$$\text{C10:} \ \theta_{ijs} + \theta_{jis} = 1, \forall i \ne j, s,$$

where r^{ot}_{ijs} is the time to adjust the attitude of AEOS s such that its sensor pointing away from target i and its transmitting antenna points at task j.

In addition, for a task, we should first use an AEOS to image it and then transmit the collected imaging data to a data receiver antenna. Toward this end, the following constraint should be satisfied:

$$\text{C11:} \sum_{\substack{t\in\mathcal{T}\\ k\in\mathcal{T}^e_{s,\mathcal{H}}}} x_{itk} t \ge \sum_{\substack{t\in\mathcal{T}\\ k\in\mathcal{O}^e_{i,s}}} x_{itk}(t + p_{ik} + r^{\text{to}}_{is}), \forall i, s,$$

where r^{to}_{is} is the time to adjust the attitude of AEOS s such that its transmitting antenna points away from task i and its sensor points at target i.

It should be noted that the binary variables λ_{ijs}, γ_{ijh}, γ_{ijh}, and θ_{ijs} are used to impose restrictions on decision variables x_{itk}, aiming to avoid sequential dependency conflicts. In particular, in the special case where two different targets i and j are not observed, the constraints C3, C5, C7, and C9 are always satisfied. Then, the right side of C4, C6, C8, and C10 can be set to zero or one. Therefore, setting them to one does not change in the optimal value of the considered problem.

3.2.3 Completed Task Constraints

Apart from the above constraints between tasks, any task should be also subjected to the following constraints:

Assignment of two types of time windows: Each task should be assigned to two time windows, both of which are associated with the same AEOS. As such, the following constraint should be satisfied:

$$\text{C12:} \sum_{\substack{t\in\mathcal{T}\\ k\in\mathcal{O}^e_{i,s}}} x_{itk} + \sum_{\substack{t\in\mathcal{T}\\ k\in\mathcal{T}^e_{s,\mathcal{H}}}} x_{itk} \ge 2 - V(1 - z_{is}), \forall i, s,$$

where $z_{is} \in \{0, 1\}$ so that $z_{is} = 1$ if task i is completed successfully by satellite s; otherwise $z_{is} = 0$. Particularly, C1, C2, and C12 ensure that a successful task should be allocated to one OTW and one TTW associated with the same AEOS.

Time window constraints: Both the start time of the observation and transmission operations for a task should be conducted within the associated time windows, i.e.,

$$\text{C13:} \sum_{\substack{t\in\mathcal{T}\\ k\in\mathcal{O}^e_{i,\mathcal{S}}}} x_{itk}a_{ik} \le \sum_{\substack{t\in\mathcal{T}\\ k\in\mathcal{O}^e_{i,\mathcal{S}}}} x_{itk}t \le \sum_{\substack{t\in\mathcal{T}\\ k\in\mathcal{O}^e_{i,\mathcal{S}}}} x_{itk}(b_{ik}-p_{ik}), \forall i,$$

$$\text{C14:} \sum_{\substack{t\in\mathcal{T}\\ k\in\mathcal{T}^e_{\mathcal{S},\mathcal{H}}}} x_{itk}a_{ik} \le \sum_{\substack{t\in\mathcal{T}\\ k\in\mathcal{T}^e_{\mathcal{S},\mathcal{H}}}} x_{itk}t \le \sum_{\substack{t\in\mathcal{T}\\ k\in\mathcal{T}^e_{\mathcal{S},\mathcal{H}}}} x_{itk}(b_{ik}-p_{ik}), \forall i.$$

3.3 Problem Formulation

Aiming to maximize the utility of ASNs, we focus on the design of the task scheduling decisions by jointly optimizing the resources of observation and transmission in ASNs. Toward this end, we formulate the problem of maximizing the weighted sum of scheduled tasks, constrained by various time windows:

$$\mathbf{P0}: \max_{(\boldsymbol{x},\boldsymbol{z},\boldsymbol{f})} \sum_{i\in\mathcal{I}}\sum_{s\in\mathcal{S}} w_i z_{is}$$
$$\text{s.t. } (\boldsymbol{x},\boldsymbol{z},\boldsymbol{f}) \in \mathcal{F}_0,$$

where $\boldsymbol{x}=\{x_{itk}\}$, $\boldsymbol{z}=\{z_{is}\}$, $\boldsymbol{f}=(\boldsymbol{\lambda},\boldsymbol{\psi},\boldsymbol{\gamma},\boldsymbol{\theta})$, $\boldsymbol{\lambda}=\{\lambda_{ijs}\}$, $\boldsymbol{\psi}=\{\psi_{ijs}\}$, $\boldsymbol{\gamma}=\{\gamma_{ijh}\}$, and $\boldsymbol{\theta}=\{\theta_{ijs}\}$. And the feasible set $\mathcal{F}_0$ is defined as:

$$\mathcal{F}_0=\left\{(\boldsymbol{x},\boldsymbol{z},\boldsymbol{f}) \;\middle|\; \begin{array}{c}\text{C1-C14}, x_{itk}\in\{0,1\},\forall i,t,k,\\ \lambda_{ijs}\in\{0,1\},\theta_{ijs}\in\{0,1\},\\ \psi_{ijs}\in\{0,1\},\forall i,j,s,\\ \gamma_{ijh}\in\{0,1\},\forall i,j,h, z_{is}\in\{0,1\},\forall i,s.\end{array}\right\}$$

The weighted sum maximization problem **P0** involves integer variables. Theorem 1 below reveals that this problem is difficult to solve in polynomial time. Therefore, we turn to investigating an approximation scheduling strategy to solve the problem.

Theorem 1. *Problem **P0** is NP-hard in general.*

Proof: The transmission scheduling problem in ASNs is the same as that of the non-agile EOSs, which is NP-hard [32]. Furthermore, we note that a special case of the observation scheduling problem in ASNs, where $p_{ik}=b_{ik}-a_{ik}$ for all i and all observation windows k, is the same as that of the non-agile EOSs, which is also NP-hard [33]. Hence, the joint observation and transmission scheduling problem in **P0** is NP-hard. This completes the proof of Theorem 1. □

4 SOLUTIONS AND ALGORITHM FRAMEWORK

In this section, we first propose an initial design using SDR to directly solve a suitably transformed version of **P0**. Next, to reduce the computation complexity, we introduce JOTSAS, a fast yet efficient joint scheduling algorithm combining the SDR method and a genetic algorithm (GA) with a conflict-driven initialization scheme.

4.1 Preliminary Design Using SDR

P0 naturally leads to an ILP. We observe that simply relaxing the integer constraints would result in a poor solution to **P0**. Therefore, we turn to a more powerful SDR approximation approach to tackle **P0**. However, despite the current form of **P0** having an intuitive physical explanation, to directly use SDR to solve **P0** will lead to a highly complex solution. More specifically, the main steps in using the SDR method to tackle **P0** are listed as follows: First, **P0** must be rewritten as a QCQP form. Second, the obtained QCQP form is reformulated into a semidefinite programming (SDP) problem. Finally, we drop the rank constraint in the SDP problem to obtain a convex semedefinite relaxation problem. Note that the binary constraint $\mathbf{x}\in\{\mathbf{0},\mathbf{1}\}$ in **P0** is equivalent to the two quadratic constraints $\mathbf{x}(\mathbf{x}-\mathbf{1})\le\mathbf{0}$ and $\mathbf{x}(\mathbf{x}-\mathbf{1})\ge\mathbf{0}$. The binary constraints $\mathbf{z}\in\{\mathbf{0},\mathbf{1}\}$ and $\mathbf{f}\in\{\mathbf{0},\mathbf{1}\}$ can be similarly transformed into quadratic constraints. After that, **P0** can be easily reformulated as a nonconvex QCQP. However, in the second step, the nonconvex QCQP achieved by the current form of **P0** is very difficult to transform into a SDP form. This motivates us to first transform **P0** into a suitable structure.

Toward this end, we leverage the inherent relation among the binary decision variables in **P0**. More specifically, it is observed that the binary decision variables in **P0** can be classified into three groups: the scheduling variable $\boldsymbol{x}$, the indicator variable $\boldsymbol{z}$, and the auxiliary variable $\boldsymbol{f}$. Particularly, $\boldsymbol{z}$ reveals the conditions of successfully scheduled tasks through the design of $\boldsymbol{x}$, while $\boldsymbol{f}$ is used to impose restriction on the scheduling decisions (i.e., $\boldsymbol{x}$) to meet the time-sequence requirements of practical observation and transmission operations. To summarize, both $\boldsymbol{z}$ and $\boldsymbol{f}$ are used to limit the value of $\boldsymbol{x}$. Inspired by this, we can remove $\boldsymbol{z}$ and $\boldsymbol{f}$ by introducing new decision variables, if they are capable of representing the same resource allocation constraints.

In what follows, by introducing new decision variables, we first remove $\boldsymbol{f}$ from **P0**, thereby obtaining new formulation **P1**. Next, by removing $\boldsymbol{z}$, we transform **P1** into a special ILP problem **P3**, which can be solved efficiently using SDR. This leads to an SDR-based scheduling algorithm to solve **P0** efficiently.

4.1.1 Reduction of Auxiliary Variable $\boldsymbol{f}$

By exploring the special structure in **P0**, we introduce new decision variables to generate a more SDR-friendly reformulation by removing $\boldsymbol{f}$. Initially, we can utilize C13 and C14 to exclude some time indices outside of time windows. That is to say, for each task, we can find all the feasible time indices within time windows (OTWs and TTWs). In particular, we need to construct one-to-one correspondence between these feasible time indices and time $t\in\mathcal{T}$. Specifically, let t^{ob}_{ink} be the time corresponding to feasible time index n within OTW k associated with task i. Similarly, t^{tr}_{imk} denotes the time corresponding to feasible time index m within TTW k associated with task i. As such, we can obtain feasible time index sets of observation and transmission, denoted by t^{ob}_{ik} and t^{tr}_{ik}, respectively, as follows:

$$t^{\text{ob}}_{ik}=\{t^{\text{ob}}_{i1k},...,t^{\text{ob}}_{iN^k_ik}\},\quad N^k_i=\left|t^{\text{ob}}_{ik}\right|,\forall i,k\in\mathcal{O}^e_{i,\mathcal{S}},$$
$$t^{\text{tr}}_{ik}=\{t^{\text{tr}}_{i1k},...,t^{\text{tr}}_{iM^k_ik}\},\quad M^k_i=\left|t^{\text{tr}}_{ik}\right|,\forall k\in\mathcal{T}^e_{\mathcal{S},\mathcal{H}}.$$

Moreover, we denote N_i and M_i as the total number of feasible observation and transmission time indices associated with task i, respectively. Thus, $N_i=\sum_{k\in\mathcal{O}^e_{i,\mathcal{S}}} N^k_i$ and

$M_i = \sum_{k \in \mathcal{T}^e_{\mathcal{S},\mathcal{H}}} M_i^k$. Next, we introduce two new decision variables $x_{t^{\text{ob}}_{ink}} \in \{0,1\}$ and $x_{t^{\text{tr}}_{imk}} \in \{0,1\}$, so that $x_{t^{\text{ob}}_{ink}} = 1$ reveals that target i is observed at time t^{ob}_{ink} corresponding to the index n within the OTW k; otherwise $x_{t^{\text{ob}}_{ink}} = 0$. Similarly, $x_{t^{\text{tr}}_{imk}} = 1$ indicates that the observation data of target i is transmitted at time t^{tr}_{imk} corresponding to the index m within the TTW k; otherwise $x_{t^{\text{tr}}_{imk}} = 0$. Therefore, the one-to-one mapping between x_{itk} and new decision variables (i.e., $x_{t^{\text{ob}}_{ink}}$ and $x_{t^{\text{tr}}_{imk}}$) is as follows:

$$x_{itk} = \begin{cases} x_{t^{\text{ob}}_{ink}}, & t^{\text{ob}}_{ink} \in t^{\text{ob}}_{ik}, k \in \mathcal{O}^e_{i,\mathcal{S}}, \\ x_{t^{\text{tr}}_{imk}}, & t^{\text{tr}}_{imk} \in t^{\text{tr}}_{ik}, k \in \mathcal{T}^e_{\mathcal{S},\mathcal{H}}. \end{cases} \tag{1}$$

Then, it is observed from C1 and C2 that a task should be allocated to at most one OTW and one TTW, respectively. Therefore, we can use the new decision variables to rewrite C1 and C2 as the following two constraints:

$$\text{C15: } \sum_{k \in \mathcal{O}^e_{i,\mathcal{S}}} \sum_{t^{\text{ob}}_{ink} \in t^{\text{ob}}_{ik}} x_{t^{\text{ob}}_{ink}} \le 1, \forall i,$$

$$\text{C16: } \sum_{k \in \mathcal{T}^e_{\mathcal{S},\mathcal{H}}} \sum_{t^{\text{tr}}_{imk} \in t^{\text{tr}}_{ik}} x_{t^{\text{tr}}_{imk}} \le 1, \forall i.$$

Next, we definite $\mathcal{A}$ as the infeasible observation set to represent some conflict observation operations in realistic applications. Specifically, according to C3 and C4, we can check whether the observation operations of any two different tasks conducted by the same satellite, e.g., $(x_{t^{\text{ob}}_{ink}}, x_{t^{\text{ob}}_{jn'k'}})$, is in conflict. If there is a conflict, we add $(t^{\text{ob}}_{ink}, t^{\text{ob}}_{jn'k'})$ into set $\mathcal{A}$. After traversing all the possible combinations, C3 and C4 can be rewritten as

$$\text{C17: } x_{t^{\text{ob}}_{ink}} + x_{t^{\text{ob}}_{jn'k'}} \le 1, \ (t^{\text{ob}}_{ink}, t^{\text{ob}}_{jn'k'}) \in \mathcal{A}.$$

Similarly, we let $\mathcal{B}$ be the infeasible transmission set to characterize the conflict transmission operations. Specifically, on the basis of C5 and C6, we can judge whether the transmission operations conducted by a satellite for any different two tasks is in conflict. Furthermore, combining C7 with C8, we can check whether the transmission operations for various tasks to access a data receiving antenna is feasible. After that, we can add all the infeasible combinations (e.g., $(t^{\text{tr}}_{imk}, t^{\text{tr}}_{jm'k'})$) unsatisfying the constraints above into set $\mathcal{B}$. As such, we can obtain the constraint as follows:

$$\text{C18: } x_{t^{\text{tr}}_{imk}} + x_{t^{\text{tr}}_{jm'k'}} \le 1, \ (t^{\text{tr}}_{imk}, t^{\text{tr}}_{jm'k'}) \in \mathcal{B}.$$

Furthermore, we denote set $\mathcal{C}$ to indicate the conflict operations between observation and transmission. Specifically, on the basis of C9-C11, we check whether the sequence of observation and transmission operations for any two different tasks on the same satellite is feasible. It follows that we can add all the infeasible combinations, e.g., $(t^{\text{ob}}_{ink}, t^{\text{tr}}_{jmk})$, into $\mathcal{C}$ to get:

$$\text{C19: } x_{t^{\text{ob}}_{ink}} + x_{t^{\text{tr}}_{jmk}} \le 1, \ (t^{\text{ob}}_{ink}, t^{\text{tr}}_{jmk}) \in \mathcal{C}.$$

Next, according to C12, we need to ensure that both the observation and transmission of a task should be on the same satellite. As such, we use the new decision variables to rewrite C12 as follows:

$$\text{C20: } \sum_{\substack{k \in \mathcal{O}^e_{i,s} \\ t^{\text{ob}}_{ink} \in t^{\text{ob}}_{ik}}} x_{t^{\text{ob}}_{ink}} + \sum_{\substack{k \in \mathcal{T}^e_{s,\mathcal{H}} \\ t^{\text{tr}}_{imk} \in t^{\text{tr}}_{ik}}} x_{t^{\text{tr}}_{imk}} \ge 2 - V(1 - z_{is}), \forall i, s.$$

Finally, the following integer constraints should be introduced:

$$\text{C21: } x_{t^{\text{ob}}_{ink}} \in \{0,1\}, t^{\text{ob}}_{ink} \in t^{\text{ob}}_{ik}, \forall i, k \in \mathcal{O}^e_{i,\mathcal{S}},$$
$$\text{C22: } x_{t^{\text{tr}}_{imk}} \in \{0,1\}, t^{\text{tr}}_{imk} \in t^{\text{tr}}_{ik}, \forall i, k \in \mathcal{T}^e_{\mathcal{S},\mathcal{H}},$$
$$\text{C23: } z_{is} \in \{0,1\}, \forall i, s.$$

By now, **P0** can be equivalently transformed into the following optimization problem:

$$\mathbf{P1}: \max_{(\boldsymbol{x}^{\text{ot}}, \boldsymbol{z})} \sum_{i \in \mathcal{I}} \sum_{s \in \mathcal{S}} w_i z_{is}$$
$$\text{s.t. } (\boldsymbol{x}^{\text{ot}}, \boldsymbol{z}) \in \mathcal{F}_1,$$

where $\boldsymbol{x}^{\text{ot}} = (\boldsymbol{x}^{\text{ob}}, \boldsymbol{x}^{\text{tr}})$, $\boldsymbol{x}^{\text{ob}} = \{x_{t^{\text{ob}}_{ink}}\}$, $\boldsymbol{x}^{\text{tr}} = \{x_{t^{\text{tr}}_{imk}}\}$, and $\mathcal{F}_1$ denotes the feasible set, defined as

$$\mathcal{F}_1 = \{ (\boldsymbol{x}^{\text{ot}}, \boldsymbol{z}) \mid \text{C15-C23} \}.$$

4.1.2 Reduction of Indicator Variable z

We first transform C20 into the following constraint:

$$z_{is} \le \frac{1}{V} \sum_{\substack{k \in \mathcal{O}^e_{i,s} \\ t^{\text{ob}}_{ink} \in t^{\text{ob}}_{ik}}} x_{t^{\text{ob}}_{ink}} + \frac{1}{V} \sum_{\substack{k \in \mathcal{T}^e_{s,\mathcal{H}} \\ t^{\text{tr}}_{imk} \in t^{\text{tr}}_{ik}}} x_{t^{\text{tr}}_{imk}} + \frac{V-2}{V}, \ \forall i, s. \tag{2}$$

Next, multiplying (2) by w_i and then summing it over both $i \in \mathcal{I}$ and $s \in \mathcal{S}$, we have

$$\begin{aligned} \sum_{i \in \mathcal{I}} \sum_{s \in \mathcal{S}} w_i z_{is} \le & \frac{1}{V} \sum_{i \in \mathcal{I}} \sum_{\substack{k \in \mathcal{O}^e_{i,\mathcal{S}} \\ t^{\text{ob}}_{ink} \in t^{\text{ob}}_{ik}}} w_i x_{t^{\text{ob}}_{ink}} \\ & + \frac{1}{V} \sum_{i \in \mathcal{I}} \sum_{\substack{k \in \mathcal{T}^e_{s,\mathcal{H}} \\ t^{\text{tr}}_{imk} \in t^{\text{tr}}_{ik}}} w_i x_{t^{\text{tr}}_{imk}} + \frac{S(V-2)}{V} \sum_{i \in \mathcal{I}} w_i. \end{aligned} \tag{3}$$

Plugging (3) into the objective of **P1** and dropping C23, we can obtain the following problem:

$$\begin{aligned} \mathbf{P2}: \max_{\boldsymbol{x}^{\text{ot}}} & \frac{1}{V} \sum_{i \in \mathcal{I}} \sum_{\substack{k \in \mathcal{O}^e_{i,\mathcal{S}} \\ t^{\text{ob}}_{ink} \in t^{\text{ob}}_{ik}}} w_i x_{t^{\text{ob}}_{ink}} + \frac{1}{V} \sum_{i \in \mathcal{I}} \sum_{\substack{k \in \mathcal{T}^e_{s,\mathcal{H}} \\ t^{\text{tr}}_{imk} \in t^{\text{tr}}_{ik}}} w_i x_{t^{\text{tr}}_{imk}} \\ & + \frac{S(V-2)}{V} \sum_{i \in \mathcal{I}} w_i \\ \text{s.t. } & \boldsymbol{x}^{\text{ot}} \in \mathcal{F}_2, \end{aligned}$$

with the feasible set $\mathcal{F}_2$ defined as

$$\mathcal{F}_2 = \{ \boldsymbol{x}^{\text{ot}} \,|\, \text{C15-C19, C21, C22}, \boldsymbol{x}^{\text{ot}} \ge \mathbf{0} \}.$$

Obviously, the optimum of **P2** is an upper bound of the optimum of **P1**, owing to the fact that the objective value of **P2** is larger than that of **P1** and $\mathcal{F}_1 \subset \mathcal{F}_2$. Furthermore, multiplying the objective of **P2** by $\frac{1}{2}V$ and then removing the constant term, we have

$$\begin{aligned} \mathbf{P3}: \max_{\boldsymbol{x}^{\text{ot}}} & \sum_{i \in \mathcal{I}} \sum_{\substack{k \in \mathcal{O}^e_{i,\mathcal{S}} \\ t^{\text{ob}}_{ink} \in t^{\text{ob}}_{ik}}} \frac{1}{2} w_i x_{t^{\text{ob}}_{ink}} + \sum_{i \in \mathcal{I}} \sum_{\substack{k \in \mathcal{T}^e_{s,\mathcal{H}} \\ t^{\text{tr}}_{imk} \in t^{\text{tr}}_{ik}}} \frac{1}{2} w_i x_{t^{\text{tr}}_{imk}} \\ \text{s.t. } & \boldsymbol{x}^{\text{ot}} \in \mathcal{F}_2. \end{aligned}$$

It is easy to understand that the optimal solution to **P3** is the same as that of **P2**. We use $\mathbf{P1}^*$ and $\mathbf{P3}^*$ to represent the optimum of **P1** and **P3**, respectively.

Theorem 2. *P3* is an upper bound of P1*. Furthermore, a necessary and sufficient condition for the equivalence of problems P1 and P3 is that in P3 each task is allocated two time windows.*

Proof: Compared with **P3**, the objective function of **P1** is bounded by the additional constraints C20 and C23. This means that, $z_{is}=1, \forall i, s$ if and only if

$$\sum_{\substack{k\in\mathcal{O}_{i,s}^e \\ t_{ink}^{\text{ob}}\in t_{ik}^{\text{ob}}}} x_{t_{ink}^{\text{ob}}} + \sum_{\substack{k\in\mathcal{T}_{s,\mathcal{H}}^e \\ t_{imk}^{\text{tr}}\in t_{ik}^{\text{tr}}}} x_{t_{imk}^{\text{tr}}} \geq 2. \tag{4}$$

Combined with C15 and C16, (4) is turned into an equality, i.e., each task should be allocated two time windows associated with the same satellite. Particularly, C19 in **P3** ensures that the OTW and TTW for a task is associated with the same satellite. As such, we only need to guarantee that each task is allocated two time windows. However, there is no such constraint in **P3**, so $\mathcal{F}_1 \subset \mathcal{F}_2$ and the objective value of **P3** over $\mathcal{F}_2$ is larger than that of **P1** over $\mathcal{F}_1$. This finishes the proof of Theorem 2. □

Remark 1. According to Theorem 2, we can convert the solution to **P3** into a feasible solution for **P1** by finding tasks associated with two time windows.

4.1.3 Preliminary SDR-based Algorithm Design

To obtain an SDR formulation, we first convert C21 and C22 into the following two constraints:

$$\text{C24: } x_{t_{ink}^{\text{ob}}}(x_{t_{ink}^{\text{ob}}}-1)=0, \quad t_{ink}^{\text{ob}} \in t_{ik}^{\text{ob}}, \forall i, k\in\mathcal{O}_{i,\mathcal{S}}^e,$$
$$\text{C25: } x_{t_{imk}^{\text{tr}}}(x_{t_{imk}^{\text{tr}}}-1)=0, \quad t_{imk}^{\text{tr}} \in t_{ik}^{\text{tr}}, \forall i, k\in\mathcal{T}_{\mathcal{S},\mathcal{H}}^e.$$

Therefore, **P3** can be transformed into an equivalent problem as follows:

$$\begin{aligned}\textbf{P4}: \max_{\boldsymbol{x}^{\text{ot}}} & \sum_{i\in\mathcal{I}}\sum_{k\in\mathcal{O}_{i,\mathcal{S}}^e}\sum_{t_{ink}^{\text{ob}}\in t_{ik}^{\text{ob}}} \frac{1}{2}w_i x_{t_{ink}^{\text{ob}}} \\ & + \sum_{i\in\mathcal{I}}\sum_{k\in\mathcal{T}_{\mathcal{S},\mathcal{H}}^e}\sum_{t_{imk}^{\text{tr}}\in t_{ik}^{\text{tr}}} \frac{1}{2}w_i x_{t_{imk}^{\text{tr}}} \\ \text{s.t. } & \text{C15-C19, C24, C25}, \boldsymbol{x}^{\text{ot}}\geq\mathbf{0}.\end{aligned}$$

Define $\boldsymbol{x}_i^{\text{ot}} = [x_{t_{i11}^{\text{ob}}}, ..., x_{t_{iN_i|\mathcal{O}_{i,\mathcal{S}}^e|}^{\text{ob}}}, x_{t_{i11}^{\text{tr}}}, ..., x_{t_{iM_i|\mathcal{T}_{\mathcal{S},\mathcal{H}}^e|}^{\text{tr}}}]^T$ as the $1\times O_i$ row vector for all i, where O_i is equal to $N_i|\mathcal{O}_{i,\mathcal{S}}^e| + M_i|\mathcal{T}_{\mathcal{S},\mathcal{H}}^e|$. It is therefore easy to obtain $\boldsymbol{x}^{\text{ot}} = [\boldsymbol{x}_1^{\text{ot}}, ..., \boldsymbol{x}_I^{\text{ot}}]^T$, which is the $1\times O$ column vector with $O=\sum_{i\in\mathcal{I}} O_i$. Moreover, $\boldsymbol{e}_{1\times N_i^k}^p$ and $\boldsymbol{e}_{1\times O_i}^p$ represent N_i^k-dimensional and O_i-dimensional column unit vectors, respectively, with the pth element being one. As such, we equivalently convert **P4** into the vector form as follows:

$$\begin{aligned}\textbf{P5}: \max_{\boldsymbol{x}^{\text{ot}}} & \sum_{i\in\mathcal{I}} (\mathbf{D}_i)^T \boldsymbol{x}_i^{\text{ot}} \\ \text{s.t. } & \left(\mathbf{b}_i^{\text{ob}}\right)^T \boldsymbol{x}_i^{\text{ot}} \leq 1, \ \left(\mathbf{b}_i^{\text{tr}}\right)^T \boldsymbol{x}_i^{\text{ot}} \leq 1, \forall i, \\ & \left(\boldsymbol{b}_{ink}^{\mathcal{A}}\right)^T \boldsymbol{x}_i^{\text{ot}} + \left(\boldsymbol{b}_{jn'k'}^{\mathcal{A}}\right)^T \boldsymbol{x}_j^{\text{ot}} \leq 1, \ \left(t_{ink}^{\text{ob}}, t_{jn'k'}^{\text{ob}}\right)\in\mathcal{A}, \\ & \left(\boldsymbol{b}_{imk}^{\mathcal{B}}\right)^T \boldsymbol{x}_i^{\text{ot}} + \left(\boldsymbol{b}_{jm'k'}^{\mathcal{B}}\right)^T \boldsymbol{x}_j^{\text{ot}} \leq 1, \ (t_{imk}^{\text{tr}}, t_{jm'k'}^{\text{tr}})\in\mathcal{B}, \\ & \left(\boldsymbol{b}_{ink}^{\mathcal{C}}\right)^T \boldsymbol{x}_i^{\text{ot}} + \left(\boldsymbol{b}_{jmk}^{\mathcal{C}}\right)^T \boldsymbol{x}_j^{\text{ot}} \leq 1, \ \left(t_{ink}^{\text{ob}}, t_{jmk}^{\text{tr}}\right)\in\mathcal{C}, \\ & (\boldsymbol{x}_i^{\text{ot}})^T \text{diag}\left(\boldsymbol{e}_{1\times O_i}^p\right) \boldsymbol{x}_i^{\text{ot}} - \left(\boldsymbol{e}_{1\times O_i}^p\right)^T \boldsymbol{x}_i^{\text{ot}} = 0, p\in\{1,...,O_i\}, \forall i, \\ & \boldsymbol{x}_i^{\text{ot}} \geq \mathbf{0}, \forall i,\end{aligned}$$

where

$$\begin{aligned}&\boldsymbol{D}_i = \frac{1}{2}w_i\mathbf{1}_{O_i\times 1}, \ \boldsymbol{b}_i^{\text{ob}} = [\mathbf{1}_{1\times N_i|\mathcal{O}_{i,\mathcal{S}}^e|}, \mathbf{0}_{1\times M_i|\mathcal{T}_{\mathcal{S},\mathcal{H}}^e|}]^T, \\ &\boldsymbol{b}_i^{\text{tr}} = [\mathbf{0}_{1\times N_i|\mathcal{O}_{i,\mathcal{S}}^e|}, \mathbf{1}_{1\times M_i|\mathcal{T}_{\mathcal{S},\mathcal{H}}^e|}]^T, \\ &\boldsymbol{b}_{ink}^{\mathcal{A}} = [\mathbf{0}_{1\times N_i^1}, ..., \boldsymbol{e}_{1\times N_i^k}^{n'}, ..., \mathbf{0}_{1\times M_i|\mathcal{T}_{\mathcal{S},\mathcal{H}}^e|}]^T, \\ &\boldsymbol{b}_{jn'k'}^{\mathcal{A}} = [\mathbf{0}_{1\times N_j^1}, ..., \boldsymbol{e}_{1\times N_j^{k'}}^{n'}, ..., \mathbf{0}_{1\times M_j|\mathcal{T}_{\mathcal{S},\mathcal{H}}^e|}]^T, \\ &\boldsymbol{b}_{imk}^{\mathcal{B}} = [\mathbf{0}_{1\times N_i|\mathcal{O}_{i,\mathcal{S}}^e|}, ..., \boldsymbol{e}_{1\times N_i^k}^{m}, ..., \mathbf{0}_{1\times M_i|\mathcal{T}_{\mathcal{S},\mathcal{H}}^e|}]^T, \\ &\boldsymbol{b}_{jm'k'}^{\mathcal{B}} = [\mathbf{0}_{1\times N_j|\mathcal{O}_{j,\mathcal{S}}^e|}, ..., \boldsymbol{e}_{1\times N_j^{k'}}^{m'}, ..., \mathbf{0}_{1\times M_j|\mathcal{T}_{\mathcal{S},\mathcal{H}}^e|}]^T, \\ &\boldsymbol{b}_{ink}^{\mathcal{C}} = [\mathbf{0}_{1\times N_i^1}, ..., \boldsymbol{e}_{1\times N_i^k}^{n}, ..., \mathbf{0}_{1\times M_i|\mathcal{T}_{\mathcal{S},\mathcal{H}}^e|}]^T, \\ &\boldsymbol{b}_{jmk}^{\mathcal{C}} = [\mathbf{0}_{1\times N_j|\mathcal{O}_{j,\mathcal{S}}^e|}, ..., \boldsymbol{e}_{1\times N_j^k}^{m}, ..., \mathbf{0}_{1\times M_j|\mathcal{T}_{\mathcal{S},\mathcal{H}}^e|}]^T.\end{aligned}$$

We further define $\boldsymbol{q}_i = [(\boldsymbol{x}_i^{\text{ot}})^T, 1]^T$ and recast **P5** as the following QCQP formulation:

$$\begin{aligned}\textbf{P6}: \max_{\{\boldsymbol{q}_i\}} & \sum_{i\in\mathcal{I}} \boldsymbol{q}_i^T \boldsymbol{G}_i \boldsymbol{q}_i \\ \text{s.t. } & \boldsymbol{q}_i^T \boldsymbol{G}_i^{\text{ob}} \boldsymbol{q}_i \leq 1, \boldsymbol{q}_i^T \boldsymbol{G}_i^{\text{tr}} \boldsymbol{q}_i \leq 1, \forall i, \\ & \boldsymbol{q}_i^T \boldsymbol{G}_{ink}^{\mathcal{A}} \boldsymbol{q}_i + \boldsymbol{q}_j^T \boldsymbol{G}_{jn'k'}^{\mathcal{A}} \boldsymbol{q}_j \leq 1, \ \left(t_{ink}^{\text{ob}}, t_{jn'k'}^{\text{ob}}\right)\in\mathcal{A}, \\ & \boldsymbol{q}_i^T \boldsymbol{G}_{imk}^{\mathcal{B}} \boldsymbol{q}_i + \boldsymbol{q}_j^T \boldsymbol{G}_{jm'k'}^{\mathcal{B}} \boldsymbol{q}_j \leq 1, \ (t_{imk}^{\text{tr}}, t_{jm'k'}^{\text{tr}})\in\mathcal{B}, \\ & \boldsymbol{q}_i^T \boldsymbol{G}_{ink}^{\mathcal{C}} \boldsymbol{q}_i + \boldsymbol{q}_j^T \boldsymbol{G}_{jmk}^{\mathcal{C}} \boldsymbol{q}_j \leq 1, \ \left(t_{ink}^{\text{ob}}, t_{jmk}^{\text{tr}}\right)\in\mathcal{C}, \\ & \boldsymbol{q}_i^T \boldsymbol{G}_p \boldsymbol{q}_i = 0, p\in\{1,...,O_i\}, \ \boldsymbol{q}_i \geq \mathbf{0}, \forall i,\end{aligned}$$

where

$$\boldsymbol{G}_{ink}^{\mathcal{A}} = \begin{bmatrix} \mathbf{0} & \frac{1}{2}\boldsymbol{b}_{ink}^{\mathcal{A}} \\ \frac{1}{2}(\boldsymbol{b}_{ink}^{\mathcal{A}})^T & \mathbf{0}\end{bmatrix}, \boldsymbol{G}_{ink}^{\mathcal{C}} = \begin{bmatrix} \mathbf{0} & \frac{1}{2}\boldsymbol{b}_{ink}^{\mathcal{C}} \\ \frac{1}{2}(\boldsymbol{b}_{ink}^{\mathcal{C}})^T & \mathbf{0}\end{bmatrix},$$
$$\boldsymbol{G}_{jmk}^{\mathcal{C}} = \begin{bmatrix} \mathbf{0} & \frac{1}{2}\boldsymbol{b}_{jmk}^{\mathcal{C}} \\ \frac{1}{2}\left(\boldsymbol{b}_{jmk}^{\mathcal{C}}\right)^T & \mathbf{0}\end{bmatrix}, \boldsymbol{G}_{imk}^{\mathcal{B}} = \begin{bmatrix} \mathbf{0} & \frac{1}{2}\boldsymbol{b}_{imk}^{\mathcal{B}} \\ \frac{1}{2}(\boldsymbol{b}_{imk}^{\mathcal{B}})^T & \mathbf{0}\end{bmatrix},$$
$$\boldsymbol{G}_{jn'k'}^{\mathcal{A}} = \begin{bmatrix} \mathbf{0} & \frac{1}{2}\boldsymbol{b}_{jn'k'}^{\mathcal{A}} \\ \frac{1}{2}(\boldsymbol{b}_{jn'k'}^{\mathcal{A}})^T & \mathbf{0}\end{bmatrix}, \boldsymbol{G}_i^{\text{ob}} = \begin{bmatrix} \mathbf{0} & \frac{1}{2}\boldsymbol{b}_i^{\text{ob}} \\ \frac{1}{2}(\boldsymbol{b}_i^{\text{ob}})^T & \mathbf{0}\end{bmatrix},$$
$$\boldsymbol{G}_{jm'k'}^{\mathcal{B}} = \begin{bmatrix} \mathbf{0} & \frac{1}{2}\boldsymbol{b}_{jm'k'}^{\mathcal{B}} \\ \frac{1}{2}(\boldsymbol{b}_{jm'k'}^{\mathcal{B}})^T & \mathbf{0}\end{bmatrix}, \boldsymbol{G}_i^{\text{tr}} = \begin{bmatrix} \mathbf{0} & \frac{1}{2}\boldsymbol{b}_i^{\text{tr}} \\ \frac{1}{2}(\boldsymbol{b}_i^{\text{tr}})^T & \mathbf{0}\end{bmatrix},$$
$$\boldsymbol{G}_i = \begin{bmatrix} \mathbf{0} & \frac{1}{2}\boldsymbol{D}_i \\ \frac{1}{2}(\boldsymbol{D}_i)^T & \mathbf{0}\end{bmatrix}, \boldsymbol{G}_p = \begin{bmatrix} \text{diag}\left(\mathbf{e}_{1\times O_i}^p\right) & -\frac{1}{2}\boldsymbol{e}_{1\times O_i}^p \\ -\frac{1}{2}(\mathbf{e}_{1\times O_i}^p)^T & \mathbf{0}\end{bmatrix}.$$

So far, we have not achieved much due to the fact that **P6** is still a computationally difficult problem. Toward this end, we define $\boldsymbol{X}_i = \boldsymbol{q}_i\boldsymbol{q}_i^T, \forall i$, and then drop the rank constraint $\text{rank}(\boldsymbol{X}_i)=1, \forall i$, to obtain a standard SDR formulation as follows:

$$\begin{aligned}\textbf{P7}: \max_{\{\boldsymbol{X}_i\}} & \sum_{i\in\mathcal{I}} \text{Tr}(\boldsymbol{G}_i\boldsymbol{X}_i) \\ \text{s.t. } & \text{Tr}(\boldsymbol{G}_i^{\text{ob}}\boldsymbol{X}_i) \leq 1, \text{Tr}(\boldsymbol{G}_i^{\text{tr}}\boldsymbol{X}_i) \leq 1, \forall i, \\ & \text{Tr}(\boldsymbol{G}_{ink}^{\mathcal{A}}\boldsymbol{X}_i) + \text{Tr}(\boldsymbol{G}_{jn'k'}^{\mathcal{A}}\boldsymbol{X}_j) \leq 1, (t_{ink}^{\text{ob}}, t_{jn'k'}^{\text{ob}})\in\mathcal{A}, \\ & \text{Tr}(\boldsymbol{G}_{imk}^{\mathcal{B}}\boldsymbol{X}_i) + \text{Tr}(\boldsymbol{G}_{jm'k'}^{\mathcal{B}}\boldsymbol{X}_j) \leq 1, (t_{imk}^{\text{tr}}, t_{jm'k'}^{\text{tr}})\in\mathcal{B}, \\ & \text{Tr}(\boldsymbol{G}_{ink}^{\mathcal{C}}\boldsymbol{X}_i) + \text{Tr}(\boldsymbol{G}_{jmk}^{\mathcal{C}}\boldsymbol{X}_j) \leq 1, (t_{ink}^{\text{ob}}, t_{jmk}^{\text{tr}})\in\mathcal{C}, \\ & \text{Tr}(\boldsymbol{G}_p\boldsymbol{X}_i) = 0, p\in\{1,...,O_i\}, \forall i, \\ & \boldsymbol{X}_i(O_i+1, O_i+1) = 1, \boldsymbol{X}_i \succeq 0, \forall i.\end{aligned}$$

It is known that **P7** can be solved to obtain an optimal solution $\boldsymbol{X}^* = \{\boldsymbol{X}_i^*\}$ in polynomial time, for example, through free SDP solvers (e.g., SDPT3, SeDuMi, SDPNAL) [34].

Upon obtaining the optimal solution $\boldsymbol{X}^*$, we can utilize a randomization method to generate an approximate solution to **P5**, targeting at yielding the best optimization objective. Here, we adopt the Gaussian randomization approach proposed in [35] to generate approximate solutions. Specifically, we let R be the number of randomizations. For $r \in \{1, 2, ..., R\}$, the rth approximate solution with respect to task i, denoted by $\boldsymbol{\pi}_i^r$, can be generated according to a normal distribution with zero expectation and variance $\boldsymbol{X}_i^*$, i.e., $\boldsymbol{\pi}_i^r \sim \mathcal{N}(0, \boldsymbol{X}_i^*)$. We need to map $\boldsymbol{\pi}^r = \{\boldsymbol{\pi}_i^r\}$ into a feasible solution of **P5**, denoted by $\tilde{\boldsymbol{\pi}}^r = \{\tilde{\boldsymbol{\pi}}_i^r\}$. We first sort all elements of $\boldsymbol{\pi}^r$ in decreasing order. Next, we sequentially consider each of the sorted elements of $\boldsymbol{\pi}^r$ starting from the largest one. We set the corresponding element in $\tilde{\boldsymbol{\pi}}^r$ to 1 if doing so satisfies C15-C19; otherwise it is set to 0. Finally, we choose the best $\tilde{\boldsymbol{\pi}}^r$ among the R random realizations. Details of this preliminary SDR-based solution method, which we term SDR-JOTSAS, are given in Algorithm 1.

Algorithm 1 Preliminary SDR-based Joint Observation and Transmission Scheduling Algorithm with Agile Satellites (SDR-JOTSAS)

Initialization: $\tilde{\boldsymbol{\pi}}^r = \mathbf{0}$.
Solve **P7** to obtain optimal solution $\boldsymbol{X}^* = \{\boldsymbol{X}_i^*\}$.
for $r = 1 : R$ **do**
  for $i = 1 : I$ **do**
    Generate $\boldsymbol{\pi}_i^r \sim \mathcal{N}(0, \boldsymbol{X}_i^*)$.
  end for
end for
Sort all elements of $\boldsymbol{\pi}^r$ in decreasing order.
for $j = 1$ to the length of $\boldsymbol{\pi}^r$ **do**
  if C15-C19 are satisfied **then**
    $\tilde{\boldsymbol{\pi}}^r(j) = 1$.
  else
    $\tilde{\boldsymbol{\pi}}^r(j) = 0$.
  end if
end for
Obtain r^* by solving $\max_r \sum_{i\in\mathcal{I}} \boldsymbol{D}_i \tilde{\boldsymbol{\pi}}_i^r$.

Output: $\tilde{\boldsymbol{\pi}}^{r^*}$.

4.2 Joint Observation and Transmission Scheduling Algorithm

By utilizing the SDR technique to optimize three-dimensional variable $\boldsymbol{x}$, Algorithm 1 enables a solution in polynomial time. Nevertheless, the huge solution space still leads to high computational complexity in practical applications. Toward this end, in the following, we partition the three-dimensional variable $\boldsymbol{x}$ into two two-dimensional variables. Accordingly, the weighted sum maximization problem can be equivalently transformed into a hybrid time window association (HTWA) problem, which contains an embedded time window resource allocation (TWRA) problem. Interestingly, simple modifications of the devised SDR method in Section 4.1 is also suitable to solve the TWRA efficiently, due to the fact that it is of a similar form of **P0**. More importantly, solving the TWRA over a smaller solution space of two-dimensional variables significantly reduces the computational time. Furthermore, we devise an efficient genetic framework to solve the HTWA with low complexity.

4.2.1 Problem Decomposition

Here, we recall the decision variable $\boldsymbol{x}$ of **P0** indicates which observation/transmission time window is associated with task i and its position within the time window. To reduce the complexity of the SDR solution proposed in Section 4.1, we will now decompose $\boldsymbol{x}$ into two parts. We first associate each task with two time windows (i.e., OTW and TTW), and then decide its start time within each time window. Toward this end, we let $x_{itk} = y_{it}\eta_{ik}, \forall i, t, k$, where η_{ik} indicates that task i is associated with time window k and y_{it} denotes that task i is processed at time t. We further divide y_{it} into two variables y_{it}^{ob} and y_{it}^{tr}, representing that task i is observed and transmitted at time t, respectively. Thus, we can replace x_{itk} by the following new variables:

$$x_{itk} = \begin{cases} y_{it}^{\text{ob}}\eta_{ik}, & k \in \mathcal{O}_{i,\mathcal{S}}^e, \\ y_{it}^{\text{tr}}\eta_{ik}, & k \in \mathcal{T}_{\mathcal{S},\mathcal{H}}^e. \end{cases} \tag{5}$$

Therefore, a reformulation of **P0** with $\boldsymbol{\eta} = \{\eta_{ik}\}$ known can be written as follows (i.e., TWRA):

$$\begin{aligned}
\textbf{P8}: \max_{(\boldsymbol{y},\boldsymbol{z},\boldsymbol{f})} \ & \sum_{i\in\mathcal{I}}\sum_{s\in\mathcal{S}} w_i z_{is} \\
\text{s.t. } \text{C1}': & \sum_{t\in\mathcal{T}} y_{it}^{\text{ob}}\eta_{ik} \le 1, \forall i, \ \text{C2}': \sum_{t\in\mathcal{T}} y_{it}^{\text{tr}}\eta_{ik} \le 1, \forall i, \\
\text{C3}': & \sum_{t\in\mathcal{T}} y_{it}^{\text{ob}}\eta_{ik} t \ge \sum_{t\in\mathcal{T}} y_{jt}^{\text{ob}}\eta_{jk}(t + p_{jk}) - V\lambda_{ijs}, \forall i \ne j, s, \\
\text{C5}': & \sum_{t\in\mathcal{T}} y_{it}^{\text{tr}}\eta_{ik} t \ge \sum_{t\in\mathcal{T}} y_{jt}^{\text{tr}}\eta_{jk}(t + p_{jk}) - V\psi_{ijs}, \forall i \ne j, s, \\
\text{C7}': & \sum_{t\in\mathcal{T}} y_{it}^{\text{tr}}\eta_{ik} t \ge \sum_{t\in\mathcal{T}} y_{jt}^{\text{tr}}\eta_{jk}(t + p_{jk}) - V\gamma_{ijh}, \forall i \ne j, h, \\
\text{C9}': & \sum_{t\in\mathcal{T}} y_{it}^{\text{ob}}\eta_{ik} t \ge \sum_{t\in\mathcal{T}} y_{jt}^{\text{tr}}\eta_{jk}(t + p_{jk}) - V\theta_{ijs}, \forall i \ne j, s, \\
\text{C11}': & \sum_{t\in\mathcal{T}} y_{it}^{\text{tr}}\eta_{ik} t \ge \sum_{t\in\mathcal{T}} y_{it}^{\text{ob}}\eta_{ik}(t + p_{ik}), \forall i, s, \\
\text{C12}': & \sum_{t\in\mathcal{T}} y_{it}^{\text{ob}}\eta_{ik} + \sum_{t\in\mathcal{T}} y_{it}^{\text{tr}}\eta_{ik} \ge 2 - V(1 - z_{is}), \forall i, s, \\
\text{C13}': & \sum_{t\in\mathcal{T}} y_{it}^{\text{ob}}\eta_{ik} a_{ik} \le \sum_{t\in\mathcal{T}} y_{it}^{\text{ob}}\eta_{ik} t \le \sum_{t\in\mathcal{T}} y_{it}^{\text{ob}}\eta_{ik}(b_{ik} - p_{ik}), \forall i, \\
\text{C14}': & \sum_{t\in\mathcal{T}} y_{it}^{\text{tr}}\eta_{ik} a_{ik} \le \sum_{t\in\mathcal{T}} y_{it}^{\text{tr}}\eta_{ik} t \le \sum_{t\in\mathcal{T}} y_{it}^{\text{tr}}\eta_{ik}(b_{ik} - p_{ik}), \forall i, \\
& \boldsymbol{f} \in \mathcal{F}_3, z_{is} \in \{0,1\}, \forall i, s, y_{it}^{\text{tr}} \in \{0,1\}, y_{it}^{\text{ob}} \in \{0,1\}, \forall i, t,
\end{aligned}$$

where $\boldsymbol{y} = (y_{it}^{\text{ob}}, y_{it}^{\text{tr}})$, and we define $\mathcal{F}_3$ as follows:

$$\mathcal{F}_3 = \left\{ \boldsymbol{f} \;\middle|\; \begin{array}{c} \text{C4, C6, C8, C10,} \\ \lambda_{ijs} \in \{0,1\}, \psi_{ijs} \in \{0,1\}, \\ \gamma_{ijh} \in \{0,1\}, \theta_{ijs} \in \{0,1\}, \forall i, j. \end{array} \right\}$$

Furthermore, we should optimize $\boldsymbol{\eta}$ to solve the following problem (i.e., HTWA):

$$\begin{aligned}
\textbf{P9}: \max_{\boldsymbol{\eta}} \ & g^*(\boldsymbol{\eta}) \\
\text{s.t. C26}: & \sum_{k\in\mathcal{O}_{i,\mathcal{S}}^e} \eta_{ik} \le 1, \sum_{k\in\mathcal{T}_{\mathcal{S},\mathcal{H}}^e} \eta_{ik} \le 1, \forall i,
\end{aligned}$$

$$\text{C27: } \sum_{k\in\mathcal{O}^e_{i,s}} \eta_{ik} + \sum_{k\in\mathcal{T}^e_{s,\mathcal{H}}} \eta_{ik} = 2, \forall i, s,$$
$$\text{C28: } \eta_{ik} \in \{0,1\}, \forall i, k,$$

where $g^*(\boldsymbol{\eta})$ is the optimal value of **P8** given $\boldsymbol{\eta}$.

Thus, **P0** can be equivalently decoupled into a high-level master problem nested by a lower-level subproblem. At the lower level, optimize $(\boldsymbol{y}, \boldsymbol{z}, \boldsymbol{f})$ when fixing $\boldsymbol{\eta}$, by solving **P8**. At the higher level, optimize $\boldsymbol{\eta}$ by solving **P9**.

4.2.2 TWRA Problem Solving

We observe that **P8** has a similar form to **P0**, so that the SDR-based solution in Section 4.1 similarly applies. However, by replacing the three-dimensional variable $\boldsymbol{x}$ by the two-dimensional variable $\boldsymbol{y}$, we can now much more efficiently solve **P8**. For clarity, we explain the mainly modifications as follows.

Initially, we recast **P8** as the following problem:

$$\begin{aligned}
\mathbf{P1}'\text{: } &\max_{(\boldsymbol{y}^{\text{ot}}, \boldsymbol{z})} \sum_{i\in\mathcal{I}}\sum_{s\in\mathcal{S}} w_i z_{is} \\
\text{s.t. C15}'\text{: } &\sum_{t^{\text{ob}}_{in}\in t^{\text{ob}}_i} y_{t^{\text{ob}}_{in}} \le 1, \forall i, \\
\text{C16}'\text{: } &\sum_{t^{\text{tr}}_{im}\in t^{\text{tr}}_i} y_{t^{\text{tr}}_{im}} \le 1, \forall i, \\
\text{C17}'\text{: } &y_{t^{\text{ob}}_{in}} + y_{t^{\text{ob}}_{jn'}} \le 1,\ (t^{\text{ob}}_{in}, t^{\text{ob}}_{jn'}) \in \mathcal{A}', \\
\text{C18}'\text{: } &y_{t^{\text{tr}}_{im}} + y_{t^{\text{tr}}_{jm'}} \le 1,\ (t^{\text{tr}}_{im}, t^{\text{tr}}_{jm'}) \in \mathcal{B}', \\
\text{C19}'\text{: } &y_{t^{\text{ob}}_{in}} + y_{t^{\text{tr}}_{jm}} \le 1,\ (t^{\text{ob}}_{in}, t^{\text{tr}}_{jm}) \in \mathcal{C}', \\
\text{C20}'\text{: } &\sum_{t^{\text{ob}}_{in}\in t^{\text{ob}}_i} y_{t^{\text{ob}}_{in}} + \sum_{t^{\text{tr}}_{im}\in t^{\text{tr}}_i} y_{t^{\text{tr}}_{im}} \ge 2 - V(1-z_{is}), \forall i, \\
\text{C21}'\text{: } &y_{t^{\text{ob}}_{in}} \in \{0,1\}, \quad t^{\text{ob}}_{in} \in t^{\text{ob}}_{ik}, \forall i, \\
\text{C22}'\text{: } &y_{t^{\text{tr}}_{im}} \in \{0,1\}, \quad t^{\text{tr}}_{im} \in t^{\text{tr}}_{ik}, \forall i, \\
\text{C23}'\text{: } &z_{is} \in \{0,1\}, \forall i,
\end{aligned}$$

where $\boldsymbol{y}^{\text{ot}} = (\boldsymbol{y}^{\text{ob}}, \boldsymbol{y}^{\text{tr}})$, $\boldsymbol{y}^{\text{ob}} = \{y_{t^{\text{ob}}_{in}}\}$, and $\boldsymbol{y}^{\text{tr}} = \{y_{t^{\text{tr}}_{im}}\}$. Obviously, **P1**′ is easy to obtain by specifying time window index k for task i in **P1**. We let $t^{\text{ob}}_i = \{t^{\text{ob}}_{in}\}$ and $t^{\text{tr}}_i = \{t^{\text{tr}}_{in}\}$, where t^{ob}_{in} and t^{tr}_{in} correspond to the values of t^{ob}_{ink} and t^{tr}_{ink} in **P1** when given $\eta_{ik}, \forall i, k$, respectively. Similarly, $y_{t^{\text{ob}}_{in}}$ and $y_{t^{\text{tr}}_{im}}$ correspond to the values of $x_{t^{\text{ob}}_{ink}}$ and $x_{t^{\text{tr}}_{imk}}$, respectively, when given $\eta_{ik}, \forall i, k$. Furthermore, according to Section 4.1.1, we construct sets $\mathcal{A}$, $\mathcal{B}$, and $\mathcal{C}$ with the known $\eta_{ik}, \forall i, k$, denoted by $\mathcal{A}'$, $\mathcal{B}'$, and $\mathcal{C}'$.

Then, removing $\boldsymbol{z}$ from **P1**′ yields the following:

$$\begin{aligned}
\mathbf{P3}'\text{: } &\max_{\boldsymbol{y}^{\text{ot}}} \sum_{i\in\mathcal{I}}\sum_{t^{\text{ob}}_{in}\in t^{\text{ob}}_i} \frac{1}{2} w_i y_{t^{\text{ob}}_{in}} + \sum_{i\in\mathcal{I}}\sum_{t^{\text{tr}}_{im}\in t^{\text{tr}}_i} \frac{1}{2} w_i y_{t^{\text{tr}}_{im}} \\
&\text{s.t. } \boldsymbol{y}^{\text{ot}} \in \mathcal{F}_2',
\end{aligned}$$

where $\mathcal{F}_2' = \left\{ \boldsymbol{y}^{\text{ot}} \middle| \text{C15}'\text{-C19}', \text{C21}', \text{C22}', \boldsymbol{y}^{\text{ot}} \ge \mathbf{0} \right\}$. Next, **P3**′ can be rewritten in the following QCQP formulation:

$$\begin{aligned}
\mathbf{P4}'\text{: } &\max_{\boldsymbol{y}^{\text{ot}}} \sum_{i\in\mathcal{I}}\sum_{t^{\text{ob}}_{in}\in t^{\text{ob}}_i} \frac{1}{2} w_i y_{t^{\text{ob}}_{in}} + \sum_{i\in\mathcal{I}}\sum_{t^{\text{tr}}_{im}\in t^{\text{tr}}_i} \frac{1}{2} w_i y_{t^{\text{tr}}_{im}} \\
&\text{s.t. C15}'\text{-C19}', \\
&\text{C24}'\text{: } y_{t^{\text{ob}}_{in}} (y_{t^{\text{ob}}_{in}} - 1) = 0, \quad t^{\text{ob}}_{in} \in t^{\text{ob}}_{ik}, \forall i, \\
&\text{C25}'\text{: } y_{t^{\text{tr}}_{im}} (y_{t^{\text{tr}}_{im}} - 1) = 0, \quad t^{\text{tr}}_{im} \in t^{\text{tr}}_{ik}, \forall i, \\
&\boldsymbol{y}^{\text{ot}} \ge \mathbf{0}.
\end{aligned}$$

Naturally, we write the vector form of **P4**′ as:

$$\begin{aligned}
\mathbf{P5}'\text{: } &\max_{\boldsymbol{y}^{\text{ot}}} \sum_{i\in\mathcal{I}} (\mathbf{D}_i')^T \boldsymbol{y}_i^{\text{ot}} \\
\text{s.t. } &\left(\mathbf{b}_i^{\text{ob}'}\right)^T \boldsymbol{y}_i^{\text{ot}} \le 1, \ \left(\mathbf{b}_i^{\text{tr}'}\right)^T \boldsymbol{y}_i^{\text{ot}} \le 1, \forall i, \\
&\left(\boldsymbol{b}_{in}^{\mathcal{A}'}\right)^T \boldsymbol{y}_i^{\text{ot}} + \left(\boldsymbol{b}_{jn'}^{\mathcal{A}'}\right)^T \boldsymbol{y}_j^{\text{ot}} \le 1, \ \left(t^{\text{ob}}_{in}, t^{\text{ob}}_{jn'}\right) \in \mathcal{A}', \\
&\left(\boldsymbol{b}_{im}^{\mathcal{B}'}\right)^T \boldsymbol{y}_i^{\text{ot}} + \left(\boldsymbol{b}_{jm'}^{\mathcal{B}'}\right)^T \boldsymbol{y}_j^{\text{ot}} \le 1, \ \left(t^{\text{tr}}_{im}, t^{\text{tr}}_{jm'}\right) \in \mathcal{B}', \\
&\left(\boldsymbol{b}_{in}^{\mathcal{C}'}\right)^T \boldsymbol{y}_i^{\text{ot}} + \left(\boldsymbol{b}_{jm}^{\mathcal{C}'}\right)^T \boldsymbol{y}_j^{\text{ot}} \le 1, \ \left(t^{\text{ob}}_{in}, t^{\text{tr}}_{jm}\right) \in \mathcal{C}', \\
&\left(\boldsymbol{y}_i^{\text{ot}}\right)^T \text{diag}\left(\boldsymbol{e}^p_{1\times O_{ik}}\right) \boldsymbol{y}_i^{\text{ot}} - \left(\boldsymbol{e}^p_{1\times O_{ik}}\right)^T \boldsymbol{y}_i^{\text{ot}} = 0, \\
&p \in \{1, ..., O'_{ik}\}, \forall i, \ \boldsymbol{y}_i^{\text{ot}} \ge 0, \forall i,
\end{aligned}$$

where

$$\begin{aligned}
&\boldsymbol{y}^{\text{ot}} = \{\boldsymbol{y}_i^{\text{ot}}\}, \boldsymbol{y}_i^{\text{ot}} = [y_{t^{\text{ob}}_{i1}}, ..., y_{t^{\text{ob}}_{iN_i^k}}, y_{t^{\text{tr}}_{i1}}, ..., y_{t^{\text{tr}}_{iM_i^k}}]^T, \\
&O'_{ik} = N_i^k + M_i^k, \ \boldsymbol{D}_i' = \frac{1}{2} w_i \mathbf{1}_{O'_{ik}\times 1}, \\
&\boldsymbol{b}_i^{\text{ob}'} = [\mathbf{1}_{1\times N_i^k}, \mathbf{0}_{1\times M_i^k}]^T, \boldsymbol{b}_i^{\text{tr}'} = [\mathbf{0}_{1\times N_i^k}, \mathbf{1}_{1\times M_i^k}]^T, \\
&\boldsymbol{b}_{in}^{\mathcal{A}'} = [\boldsymbol{e}^n_{1\times N_i^k}, \mathbf{0}_{1\times M_i^k}]^T, \boldsymbol{b}_{jn'}^{\mathcal{A}'} = [\boldsymbol{e}^{n'}_{1\times N_j^k}, \mathbf{0}_{1\times M_j^k}]^T, \\
&\boldsymbol{b}_{im}^{\mathcal{B}'} = [\mathbf{0}_{1\times N_i^k}, \boldsymbol{e}^m_{1\times M_i^k}]^T, \boldsymbol{b}_{jm'}^{\mathcal{B}'} = [\mathbf{0}_{1\times N_j^k}, \boldsymbol{e}^{m'}_{1\times M_j^k}]^T, \\
&\boldsymbol{b}_{in}^{\mathcal{C}'} = [\boldsymbol{e}^n_{1\times N_i^k}, \mathbf{0}_{1\times M_i^k}]^T, \boldsymbol{b}_{jm}^{\mathcal{C}'} = [\boldsymbol{e}^m_{1\times N_j^k}, \mathbf{0}_{1\times M_j^k}]^T.
\end{aligned}$$

Then, let $\boldsymbol{p}_i = [(\boldsymbol{y}_i^{\text{ot}})^T, 1]^T$ and give the QCQP form of **P5**′:

$$\begin{aligned}
\mathbf{P6}'\text{: } &\max_{\boldsymbol{p}_i} \sum_{i\in\mathcal{I}} \boldsymbol{p}_i^T \boldsymbol{G}_i' \boldsymbol{p}_i \\
\text{s.t. } &\boldsymbol{p}_i^T \boldsymbol{G}_i^{\text{ob}'} \boldsymbol{p}_i \le 1, \boldsymbol{p}_i^T \boldsymbol{G}_i^{\text{tr}'} \boldsymbol{p}_i \le 1, \forall i, \\
&\boldsymbol{p}_i^T \boldsymbol{G}_{in}^{\mathcal{A}'} \boldsymbol{p}_i + \boldsymbol{p}_j^T \boldsymbol{G}_{jn'}^{\mathcal{A}'} \boldsymbol{p}_j \le 1, (t^{\text{ob}}_{in}, t^{\text{ob}}_{jn'}) \in \mathcal{A}', \\
&\boldsymbol{p}_i^T \boldsymbol{G}_{im}^{\mathcal{B}'} \boldsymbol{p}_i + \boldsymbol{p}_j^T \boldsymbol{G}_{jm'}^{\mathcal{B}'} \boldsymbol{p}_j \le 1, (t^{\text{tr}}_{im}, t^{\text{tr}}_{jm'}) \in \mathcal{B}', \\
&\boldsymbol{p}_i^T \boldsymbol{G}_{im}^{\mathcal{C}'} \boldsymbol{p}_i + \boldsymbol{p}_j^T \boldsymbol{G}_{jn}^{\mathcal{C}'} \boldsymbol{p}_j \le 1, (t^{\text{ob}}_{in}, t^{\text{tr}}_{jm}) \in \mathcal{C}', \\
&\boldsymbol{p}_i^T \boldsymbol{G}_p' \boldsymbol{p}_i = 0, p \in \{1, ..., O'_{ik}\}, \forall i, \ \boldsymbol{p}_i \ge 0, \forall i,
\end{aligned}$$

where

$$\begin{aligned}
&\boldsymbol{G}_{im}^{\mathcal{C}'} = \begin{bmatrix} \mathbf{0} & \frac{1}{2}\boldsymbol{b}_{im}^{\mathcal{C}'} \\ \frac{1}{2}(\boldsymbol{b}_{im}^{\mathcal{C}'})^T & \mathbf{0} \end{bmatrix}, \boldsymbol{G}_i^{\text{ob}'} = \begin{bmatrix} \mathbf{0} & \frac{1}{2}\boldsymbol{b}_i^{\text{ob}'} \\ \frac{1}{2}(\boldsymbol{b}_i^{\text{ob}'})^T & \mathbf{0} \end{bmatrix}, \\
&\boldsymbol{G}_i^{\text{tr}'} = \begin{bmatrix} \mathbf{0} & \frac{1}{2}\boldsymbol{b}_i^{\text{tr}'} \\ \frac{1}{2}(\boldsymbol{b}_i^{\text{tr}'})^T & \mathbf{0} \end{bmatrix}, \boldsymbol{G}_{in}^{\mathcal{A}'} = \begin{bmatrix} \mathbf{0} & \frac{1}{2}\boldsymbol{b}_{in}^{\mathcal{A}'} \\ \frac{1}{2}(\boldsymbol{b}_{in}^{\mathcal{A}'})^T & \mathbf{0} \end{bmatrix}, \\
&\boldsymbol{G}_{jn}^{\mathcal{A}'} = \begin{bmatrix} \mathbf{0} & \frac{1}{2}\boldsymbol{b}_{jn'}^{\mathcal{A}'} \\ \frac{1}{2}(\boldsymbol{b}_{jn'}^{\mathcal{A}'})^T & \mathbf{0} \end{bmatrix}, \boldsymbol{G}_{im}^{\mathcal{B}'} = \begin{bmatrix} \mathbf{0} & \frac{1}{2}\boldsymbol{b}_{im}^{\mathcal{B}'} \\ \frac{1}{2}(\boldsymbol{b}_{im}^{\mathcal{B}'})^T & \mathbf{0} \end{bmatrix}, \\
&\boldsymbol{G}_{jm'}^{\mathcal{B}'} = \begin{bmatrix} \mathbf{0} & \frac{1}{2}\boldsymbol{b}_{j,m'}^{\mathcal{B}'} \\ \frac{1}{2}(\boldsymbol{b}_{jm'}^{\mathcal{B}'})^T & \mathbf{0} \end{bmatrix}, \boldsymbol{G}_{jn}^{\mathcal{C}'} = \begin{bmatrix} \mathbf{0} & \frac{1}{2}\boldsymbol{b}_{jn}^{\mathcal{C}'} \\ \frac{1}{2}(\boldsymbol{b}_{jn}^{\mathcal{C}'})^T & \mathbf{0} \end{bmatrix}, \\
&\boldsymbol{G}_i' = \begin{bmatrix} \mathbf{0} & \frac{1}{2}\boldsymbol{D}_i' \\ \frac{1}{2}(\boldsymbol{D}_i')^T & \mathbf{0} \end{bmatrix}, \boldsymbol{G}_p' = \begin{bmatrix} \text{diag}(\mathbf{e}^p_{1\times O'_{ik}}) & -\frac{1}{2}\boldsymbol{e}^p_{1\times O'_{ik}} \\ -\frac{1}{2}(\mathbf{e}^p_{1\times O'_{ik}})^T & \mathbf{0} \end{bmatrix}.
\end{aligned}$$

Finally, define $\boldsymbol{Y}_i = \boldsymbol{p}_i \boldsymbol{p}_i^T, \forall i$, and we have the SDR formulation as follows:

$$\begin{aligned}
\mathbf{P7}'\text{: } &\max_{\boldsymbol{Y}_i} \sum_{i\in\mathcal{I}} \text{Tr}(\boldsymbol{G}_i' \boldsymbol{Y}_i) \\
&\text{s.t. } \text{Tr}(\boldsymbol{G}_i^{\text{ob}'} \boldsymbol{Y}_i) \le 1, \text{Tr}(\boldsymbol{G}_i^{\text{tr}'} \boldsymbol{Y}_i) \le 1, \forall i,
\end{aligned}$$

$$\mathrm{Tr}(\boldsymbol{G}_{in}^{\mathcal{A}'}\boldsymbol{Y}_i)+\mathrm{Tr}(\boldsymbol{G}_{jn'}^{\mathcal{A}'}\boldsymbol{Y}_j)\leq 1,(t_{in}^{\mathrm{ob}},t_{jn'}^{\mathrm{ob}})\in\mathcal{A}',$$
$$\mathrm{Tr}(\boldsymbol{G}_{im}^{\mathcal{B}'}\boldsymbol{Y}_i)+\mathrm{Tr}(\boldsymbol{G}_{jm'}^{\mathcal{B}'}\boldsymbol{Y}_j)\leq 1,(t_{im}^{\mathrm{tr}},t_{jm'}^{\mathrm{tr}})\in\mathcal{B}',$$
$$\mathrm{Tr}(\boldsymbol{G}_{im}^{\mathcal{C}'}\boldsymbol{Y}_i)+\mathrm{Tr}(\boldsymbol{G}_{jn}^{\mathcal{C}'}\boldsymbol{Y}_j)\leq 1,(t_{in}^{\mathrm{ob}},t_{jm}^{\mathrm{tr}})\in\mathcal{C}',$$
$$\mathrm{Tr}(\boldsymbol{G}_{p}'\boldsymbol{Y}_i)=0,p\in\{1,...,O_{ik}'\},\forall i,$$
$$\boldsymbol{Y}_i(O_{ik}'+1,O_{ik}'+1)=1,\boldsymbol{Y}_i\succeq 0,\forall i.$$

Similar to the initial design using SDR, the remaining steps are proceeded as follows. First, we solve $\mathbf{P7}'$ to obtain optimal solution $\boldsymbol{Y}^*=\{\boldsymbol{Y}_i^*\}$. Then, we utilize the Gaussian randomization approach to generate approximate solutions, followed by recovering them into feasible solutions. Due to page limitation, we omit the details, which can be found in Section 4.1.

4.2.3 HTWA Problem Solving

Aiming to solve **P9** efficiently, we adopt a genetic framework on the basis of generated feasible solutions. GA is a well-known approach to find near-optimal solutions to NP-hard problems through simulating the process of natural selection [36]. Our main contribution in using GA to solve the HTWA problem is in the novel CPInit method below.

The GA first represents the candidate solutions of an optimization problem as a set of chromosomes termed as a population. Then, bio-inspired operations (e.g., mutation, crossover, and selection) are made on these chromosomes targeting at evolving better solutions to the optimization problem without excessive computational effort. We utilize GA to remodel the **P9** as follows:

Chromosome Representation: A candidate solution of **P9** (i.e., $\boldsymbol{\eta}$) is represented as a chromosome, which is made up of two chromatids. We respectively term these two chromatids the observation and transmission chromatid. We use a vector of length I to represent each chromatid. Thus, we can execute chromosome coding by assigning time window indices to every element of such vector, thereby constructing the one to one mapping between $\boldsymbol{\eta}$ and a chromosome. Furthermore, we introduce fitness values to evaluate chromosomes. Specifically, we define the fitness value of a chromosome as the weighted sum of scheduled tasks denoted by g. As such, we can find its fitness value $g=g^*(\boldsymbol{\eta})$ by solving the TWRA problem **P8**.

CPInit method: An efficient population initialization is of vital importance because it can accelerate the convergence speed and also improve the quality of solution. Particularly, as pointed out by [37], seeding some possible solutions in the initial population tends to improve the performance of GA. Inspired by this view, we first use a random initialization method to an initial population in a random manner, then propose a CPInit method to solve **P3** aiming at generating a set of initial solutions, and finally seed these obtained solutions in the produced initial population.

In CPInit, we utilize the information including resource requirement conflicts and the weight of tasks to generate an initial population. Specifically, we first construct a conflict function set to quantitatively characterize the conflicts among various decision variables. Then, according to both the conflict function set and the weight of tasks, we further design a probability distribution aiming at maintaining genetic diversity. Finally, we produce an initial population according to both the conflict function set and the designed probability distribution. Detail descriptions are provided below.

Algorithm 2 Conflict-driven Population Initialization Algorithm (CPInit)

Input: Random initial population $\mathcal{P}\neq\emptyset$.
1: Calculate conflict function set $f(\boldsymbol{x}^{\mathrm{ot}})$.
2: Obtain $p(\boldsymbol{x}^{\mathrm{ot}})$ according to both (6) and $f(\boldsymbol{x}^{\mathrm{ot}})$.
3: **for** $u=1:U$ **do**
4: Obtain a solution $\bar{\boldsymbol{x}}_u$ according to $p(\boldsymbol{x}^{\mathrm{ot}})$.
5: Map $\bar{\boldsymbol{x}_u}$ into $\boldsymbol{\eta}$.
6: Obtain $\mathcal{P}_u$ from $\mathcal{P}$ and update $\mathcal{P}=\mathcal{P}\setminus\mathcal{P}_u$.
7: Seed $\boldsymbol{\eta}$ into $\mathcal{P}_u$.
8: Update $\mathcal{P}=\mathcal{P}\cup\mathcal{P}_u$.
9: **end for**
Output: $\mathcal{P}$.

Algorithm 3 Joint Observation and Transmission Scheduling Algorithm with Agile Satellites (JOTSAS)

Input: Generation number L, population size U.
1: Obtain initial population $\mathcal{P}$ of size U by calling CPInit (Algorithm 2).
2: **while** $l\leq L$ **do**
3: Execute crossover and mutation operators.
4: Map each chromosome into $\boldsymbol{\eta}$ and obtain their fitness values by solving TWRA (i.e., **P8**).
5: Use the strategies of tournament and elitism to select chromosomes according to their fitnesses.
6: $l=l+1$.
7: **end while**
8: Choose the best chromosome and then map it into $\boldsymbol{x}$.
Output: $\boldsymbol{x}$.

Step 1: Construction of conflict function set: We observe that the constraints C15-C19 of **P3** have the same structure that the sum of variables is less than one. Furthermore, this special structure combined with binary constraints (i.e., C21 and C22) reveals the special conflict relationship that at most one variable in a constraint can be set to one. To quantitatively analyze the conflicts relationship among various variables, we introduce a conflict function denoted by $f(x)$ to represent the conflicts among variable $x\in\boldsymbol{x}^{\mathrm{ot}}$ with other variables. [1] For example, say $x=x_{t_{ink}^{\mathrm{ob}}}$, we first initialize $f(x_{t_{ink}^{\mathrm{ob}}})=0$, and then let $f(x_{t_{ink}^{\mathrm{ob}}})=f(x_{t_{ink}^{\mathrm{ob}}})+1$ when finding $x_{t_{ink}^{\mathrm{ob}}}+x_{t_{j'n'k'}^{\mathrm{ob}}}=1$ according to constraints C15-C19. In addition, we define a conflict function set $f(\boldsymbol{x}^{\mathrm{ot}})=\{f(x)\}$. Obviously, a larger value of $f(x)$ reveals that variable $x\in\boldsymbol{x}^{\mathrm{ot}}$ conflicts with more other variables. Naturally, we prefer to choose variable $x\in\boldsymbol{x}^{\mathrm{ot}}$ with a smaller value of $f(x)$, to maximize the optimization objective. Accordingly, we sort the elements of $f(\boldsymbol{x}^{\mathrm{ot}})$ in the order of increasing values, while returning the number of different values denoted by Q. The elements of $\boldsymbol{x}^{\mathrm{ot}}$ are thus grouped into Q clusters. For any $q\in\{1,2,...,Q\}$, we denote by ζ_q cluster q and let $\boldsymbol{\zeta}=\{\zeta_q\}$.

Step 2: Design of population generation probability: To diversify the initial population, we focus on devising a pop-

1. For convenience, we omit the subscript of the elements of $\boldsymbol{x}^{\mathrm{ot}}$ hereinafter, i.e., using notation x instead of $x_{t_{ink}^{\mathrm{ob}}}$ or $x_{t_{imk}^{\mathrm{tr}}}$.

ulation generation probability distribution $p(\boldsymbol{x}^{\text{ot}}) = \{p(x)\}$, where $p(x)$ denotes the probability of setting variable $x \in \boldsymbol{x}^{\text{ot}}$ to one. More specifically, according to the definition of $\boldsymbol{x}^{\text{ot}}$, we can obtain a task index, say i, associated with each variable $x \in \boldsymbol{x}^{\text{ot}}$, thereby obtaining the corresponding weighted value w_i. For clarity, we introduce a weighted function $w(x)$ to indicate the mapping between variable x and w_i, thereby yielding $w(x) = w_i$. As such, for any variable x, we calculate the population generation probability as follows:

$$p(x) = \frac{w(x)}{\sum\limits_{x \in \zeta_q} w(x)}, \ \forall q. \tag{6}$$

Step 3: Generation of initial population: In this step, we use $p(\boldsymbol{x}^{\text{ot}})$ obtained by Step 2 to generate an initial population suitable for solving HTWA. We denote by $\mathcal{P} = \{\mathcal{P}_u, 1 \leq u \leq U\}$ the random initial population, where $\mathcal{P}_u$ is the uth chromosome of $\mathcal{P}$ and U is the size of $\mathcal{P}$. For any u, we first use $p(\boldsymbol{x}^{\text{ot}})$ to generate the uth solution to **P3** denoted by $\bar{\boldsymbol{x}}_u$ as follows: The elements of $\boldsymbol{x}^{\text{ot}}$ are first ordered in the natural order $1, 2, ..., Q$ of clusters, and then, for each cluster ζ_q, its elements are ordered with respect to the random numbers generated by $p(\boldsymbol{x}^{\text{ot}})$. Finally, we set the variables $x \in \boldsymbol{x}^{\text{ot}}$ to one sequentially according to the above order, while obeying constraints C15-C19; otherwise zero.

Then, we map $\bar{\boldsymbol{x}}_u$ into $\boldsymbol{\eta}$ combining (1) with $\bar{x}_{itk} = y_{it}\eta_{ik}$. Finally, we seed $\boldsymbol{\eta}$ into $\mathcal{P}_u$. More specifically, for all $\eta_{ik} \in \boldsymbol{\eta}$, we find the task index i and time window index k satisfying $\eta_{ik} = 1$. If window k is an OTW, we set the ith element of the observation chromatid in $\mathcal{P}_u$ to k; otherwise, set the ith element of the transmission chromatid in $\mathcal{P}_u$ to k. The execution of these steps for exactly U times generates our initial population.

5 SIMULATION EVALUATION

In this section, we evaluate the performance of the proposed algorithm (i.e., JOTSAS) via a co-simulation platform using Matlab and the Satellite Tool Kit (STK).

TABLE II. Simulation Parameters

Data collectors	Inclination	LTDN	Altitude
AEOS 1	98.50°	10:30	778 km
AEOS 2	98.87°	08:34	863 km
AEOS 3	98.48°	13:30	770 km
Data sinks	**Latitude**	**Longitude**	
DRS 1	0°	275°	
DRS 2	0°	46.2°	
DRS 3	0°	174°	
KaShi	39.5°	76°	
SanYa	18°	109.5°	
MiYun	40.0°	116.0°	
Target distribution	**Latitude range**	**Longitude range**	
Small area	$[3°, 13°]$	$[73°, 83°]$	
Medium area	$[3°, 53°]$	$[74°, 133°]$	
Big area	$[0°, 60°]$	$[-120°, -60°]$	

LTDN is the abbreviation for "local time of descending node".

5.1 Parameters Setting

In the simulation, we set data collectors to three AEOSs. All the data sinks consist of three data relay satellites (DRSs) and three GSs. The relevant parameters of data sinks, AEOSs, and target distribution are summarized in TABLE II. Each DRS is equipped with one single-access antenna, whose transmission rate is set to 20 Mbit/s. The transmission rate of communication links between the AEOSs and GSs, denoted by R^{tr}, is set to 40 Mbit/s. The width of OTWs, denoted by α, is set to 120 seconds [38]. The imaging time of each target is 30 seconds [39]. The size of slot is set to 10 seconds. The data amount of each image is 10 Gbits. Also, each task is associated with a weight, generated with an uniformly distribution on the interval $[1, 10]$. The parameters of r^{oo}_{ijs}, r^{tt}_{ijs}, l_{ijh}, r^{ot}_{ijs}, and r^{to}_{is} are set to zeros. In GA, we set the mutation probability, crossover probability, and population size to 0.8, 0.5, and 60, respectively. The number of genetic generations is set to 400. The scheduling time horizon is from 1 May 2019 00:00:00 to 1 May 2019 12:00:00. We use the Matlab toolbox YALMIP to call the solver SDPNAL to solve the SDR problems. We adopt the target distribution with medium area and data sinks consisting of three GSs (i.e., Kashi, SanYa, and MiYun) in the following experiments, unless otherwise stated.

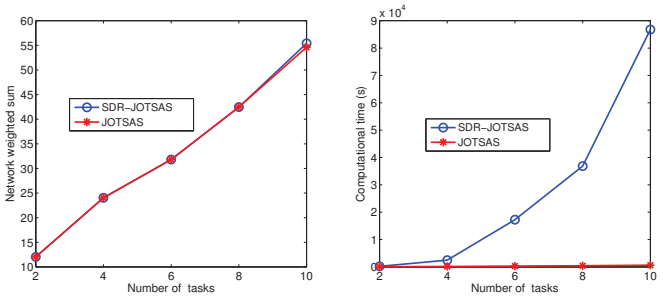

(a) Comparisons in terms of the weighted sum of scheduled tasks. (b) Comparisons in terms of computational time.

Fig. 3. Comparison between SDR-JOTSAS and JOTSAS.

5.2 Benefit of JOTSAS over Preliminary SDR-JOTSAS

We first study the benefit of JOTSAS over our preliminary design SDR-JOTSAS, which solves **P0** directly. Fig. 3a compares the two designs in terms of the weighted sum of scheduled tasks. It shows that they give nearly identical performance. Meanwhile, in Fig. 3b, we plot the computational time versus the number of tasks. It can be seen that the computational time of SDR-JOTSAS is much higher. This is because the number of time windows (including OTWs and TTWs) increases significantly over the number of tasks, thereby leading to exacerbating resource assignment conflicts, such that the number of constraints in **P3** grows exceedingly large. Thus, JOTSAS is a superior algorithm incorporating the low-complexity of GA and high efficiency of SDR.

5.3 Impact of Design Elements in JOTSAS

In the proposed discretization model, we discretize the continuous time line into T intervals, which may resulting some performance loss. To quantify it, we have plotted Fig. 4 to illustrate the weighted sum of the scheduled tasks versus the slot size. It is observed from Fig. 4 that the performance loss is negligible when the slot size is below 20 seconds in our practical setting.

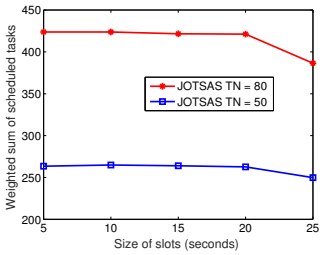

Fig. 4. Weighted sum of scheduled tasks versus slot size.

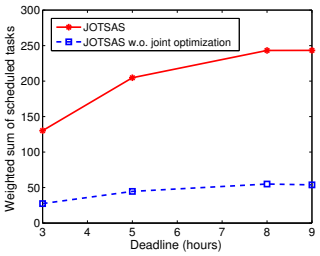

Fig. 6. Comparison between JOTSAS and JOTASA without joint optimization.

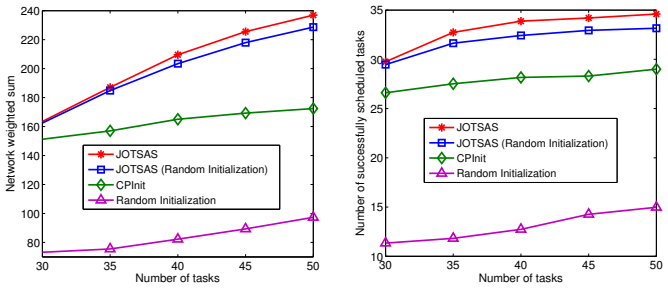

(a) Weighted sum of scheduled tasks versus the number of tasks.

(b) Number of successfully scheduled tasks versus the number of tasks.

Fig. 5. Verification of population initialization in medium area scenario.

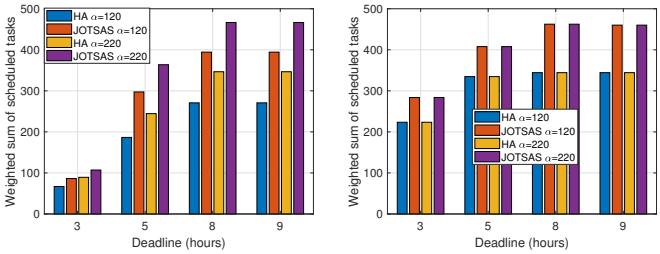

(a) Small-area scenario.

(b) Big-area scenario.

Fig. 7. Comparison of the weighted sum of scheduled tasks versus deadline.

We further study the impact of the CPInit population initialization method in JOTSAS. For this purpose, we compare it with an alternative random initialization method, where for any task i, set $x_{t^{\text{ob}}_{iN_i^k|\mathcal{O}^e_{i,\mathcal{S}}|}} = 1$ with the probability of $\frac{1}{N_i|\mathcal{O}^e_{i,\mathcal{S}}|}, \forall k \in \mathcal{O}^e_{i,\mathcal{S}}$ and set $x_{t^{\text{tr}}_{iM_i^k|\mathcal{T}^e_{\mathcal{S},\mathcal{H}}|}} = 1$ with the probability of $\frac{1}{M_i|\mathcal{T}^e_{\mathcal{S},\mathcal{H}}|}, \forall k \in \mathcal{T}^e_{\mathcal{S},\mathcal{H}}$.

Fig. 5 shows how the weighted sum of scheduled tasks and the number of successfully scheduled tasks vary with task number in various schemes. Here, we use *CPInit* and *Random Initialization* to label the solutions generated by these two methods without further GA refinement. From Fig. 5, we observe that CPInit substantially outperforms the random initialization method. This is because CPInit utilizes information involving resource requirement conflicts and the weight of tasks to devise a probability distribution, thereby capable of yielding a superior solution. Furthermore, the performance of JOTSAS is superior to its random initialization version. This indicates that CPInit provides an excellent initial population, thereby improving the quality of the final solution.

5.4 Performance Comparisons of JOTSAS and Alternatives

To reveal the benefit of joint resource optimization, we further compare JOTSAS with a naive alternative, where the observation and transmission resources are optimized separately by using JOTSAS. In Fig. 6, we show the results of this comparison, in terms of the weighted sum of scheduled tasks versus deadline. This figure suggests that joint scheduling of observation and transmission can significantly improve the performance of ASNs.

In this subsection, we compare the performance of JOTSAS with that of the heuristic algorithm (HA) devised by [26]. We set the number of tasks to 100 and $R^{\text{tr}} = 100$ Mbit/s. Furthermore, we present two scenarios to test the performance of JOTSAS. In particular, we adopt DRS 1, Kashi, SanYa, and MiYun for data sinks to guarantee enough transmission resources in the small-area scenario.

Fig. 7 compares JOTSAS with HA for different sizes of OTWs and deadlines in terms of the weighted sum of scheduled tasks. From Fig. 7(a), we observe that both JOTSAS and HA with the larger value of α achieve a lager weighted sum of scheduled tasks. This is because a larger OTW alleviates the observation conflicts within it. In addition, it is observed from Fig. 7(a) that JOTSAS achieves significantly better performance than HA. This is because the small-area scenario reinforces the overlap among various OTWs, thereby significantly exacerbating the observation conflicts. Furthermore, the transmission resources are sufficient to download the imaging data of scheduled tasks in the small area scenario. Particularly, JOTSAS enables the start time to image each target at any time within its associated OTWs, thereby significantly reducing observation conflicts.

Moreover, Fig. 7(b) shows that JOTSAS still outperforms HA in the big-area scenario. This is because JOTSAS is capable of efficiently allocating transmission resources. In this scenario, the observation conflicts are not obvious, while the transmission conflicts are intense. Nevertheless, JOTSAS jointly schedules observation and transmission resources to significantly boost the performance of ASNs.

To further verify the performance of JOTSAS, a approximate multi-resource schedule (AMRS) proposed in [22] is adopted as a baseline algorithm in an experiment with a

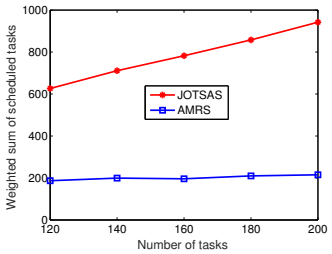

Fig. 8. Comparison between JOTSAS and AMRS in terms of the weighted sum of scheduled tasks.

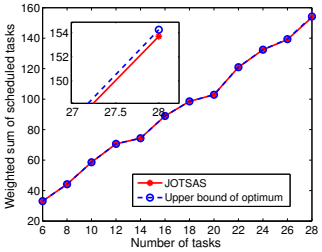

Fig. 9. Performance gap between JOTSAS and the upper bound of optimum.

larger number of tasks. In particular, AMRS is proposed to solve the problem of integrated observation and transmission scheduling in non-agile EOSs. That is, AMRS can be considered a simple approach with one pitching angle of AEOSs. Therefore, it can be used in our joint scheduling problem. In Fig. 8, we compare JOTSAS with AMRS in terms of the weighted sum of scheduled tasks versus the number of tasks. It is observed from Fig. 8 that JOTSAS outperforms AMRS in terms of the weighted sum of scheduled tasks. This is because JOTSAS coordinates multiple pitching angles of AEOSs to reduce observation conflicts, thereby facilitating observation data collection. It is therefore that AEOSs have a higher network performance over non-agile EOSs.

We plot Fig. 9 to check the performance gap between JOTSAS and an upper bound of optimum with various task number. The upper bound of optimum is obtained through the following two steps: First, we use the software STK to calculate the set of targets successfully observed by the AEOSs. Then, we calculate the weighted sum of these targets. As shown in Fig. 9, we observe that the performance gap is small.

6 Conclusion

In this paper, we have investigated the joint resource scheduling problem considering observation and transmission time windows for ASNs. Specifically, we formulate the studied problem as a weighted sum maximization problem under the constraint of diverse time windows through joint optimization of observation and transmission resources. To tackle this problem, we first utilize the SDR method to devise a joint resource scheduling algorithm, termed SDR-JOTSAS. Then, to reduce the computation complexity, we further develope a fast yet efficient joint scheduling algorithm, termed JOTSAS, through combining parts of SDR-JOTSAS and a GA approach that utilizes a new method for population initialization. Our simulation results exhibit the performance advantage of JOTSAS and the impact of its design components.

References

[1] J. Du, C. Jiang, Q. Guo, M. Guizani, and Y. Ren, "Cooperative earth observation through complex space information networks," *IEEE Wireless Commun.*, vol. 23, no. 2, pp. 136–144, Apr. 2016.

[2] L. Zhao, X. Wu, Y. Liu, and Y. Hao, "A segmented attitude planning and controlling method for agile satellite based on pseudospectral method," *Trans. Inst. Meas. Control.*, vol. 40, no. 4, pp. 1188–1200, 2018.

[3] C. Lynnes, "Advanced analytics and big earth data," NASA Goddard Space Flight Center, Washington, DC, United States, Oral/Visual Presentation, Sept. 2018.

[4] F. Hu, C. Yang, J. L. Schnase, D. Q. Duffy, M. Xu, M. K. Bowen, T. Lee, and W. Song, "Climatespark: An in-memory distributed computing framework for big climate data analytics," *Comput. and Geosci.*, vol. 115, pp. 154–166, Jun. 2018.

[5] S. E. Burrowbridge, "Optimal allocation of satellite network resources," Ph.D. dissertation, Virginia Polytechnic Institute and State University, Dec. 1999.

[6] X. Wang, G. Wu, L. Xing, and W. Pedrycz, "Agile earth observation satellite scheduling over 20 years: Formulations, methods, and future directions," *IEEE Syst. J.*, 2020.

[7] P. Tangpattanakul, N. Jozefowiez, and P. Lopez, "A multi-objective local search heuristic for scheduling earth observations taken by an agile satellite," *Eur. J. Oper. Res.Oper.*, vol. 245, no. 2, pp. 542–554, Sept. 2015.

[8] G. Li, C. Chen, F. Yao, R. He, and Y. Chen, "Hybrid differential evolution optimisation for earth observation satellite scheduling with time-dependent earliness-tardiness penalties," *Math. Probl. Eng.*, Aug. 2017.

[9] X. Liu, G. Laporte, Y. Chen, and R. He, "An adaptive large neighborhood search metaheuristic for agile satellite scheduling with time-dependent transition time," *Comput. Oper. Res.*, vol. 86, pp. 41–53, Oct. 2017.

[10] J. Lu, Y. Chen, and R. He, "A learning-based approach for agile satellite onboard scheduling," *IEEE Access*, vol. 8, pp. 16 941–16 952, 2020.

[11] L. He, X. Liu, G. Laporte, Y. Chen, and Y. Chen, "An improved adaptive large neighborhood search algorithm for multiple agile satellites scheduling," *Comput. Oper. Res.*, vol. 100, pp. 12–25, Dec. 2018.

[12] L. He, X. Liu, Y. Chen, L. Xing, and K. Liu, "Hierarchical scheduling for real-time agile satellite task scheduling in a dynamic environment," *Adv. Space Res.*, Oct. 2018.

[13] H. Chao, X. Wang, G. Song, and R. Leus, "Scheduling multiple agile earth observation satellites with multiple observations," *eprint arXiv:1812.00203*, Dec. 2018.

[14] L. Li, H. Chen, J. Li, N. Jing, and M. Emmerich, "Preference-based evolutionary many-objective optimization for agile satellite mission planning," *IEEE Access*, vol. 6, pp. 40 963–40 978, Jul. 2018.

[15] Y. He, L. Xing, Y. Chen, W. Pedrycz, L. Wang, and G. Wu, "A generic markov decision process model and reinforcement learning method for scheduling agile earth observation satellites," *IEEE Trans. Syst., Man, Cybern.: Syst.*, 2020.

[16] J. Wang, D. Erik, X. Hu, and G. Wu, "Expectation and SAA models and algorithms for scheduling of multiple earth observation satellites under the impact of clouds," *IEEE Syst. J.*, 2020.

[17] X. Jia, T. Lv, F. He, and H. Huang, "Collaborative data downloading by using inter-satellite links in LEO satellite networks," *IEEE Trans. Wireless Commu.*, vol. 16, no. 3, pp. 1523–1532, Mar. 2017.

[18] B. Deng, C. Jiang, L. Kuang, S. Guo, J. Lu, and S. Zhao, "Two-phase task scheduling in data relay satellite systems," *IEEE Trans. Veh. Technol.*, vol. 67, no. 2, pp. 1782–1793, Feb. 2018.

[19] L. He, J. Li, M. Sheng, R. Liu, K. Guo, and J. Liu, "Joint allocation of transmission and computation resources for space networks," in *Proc. IEEE WCNC*, Apr. 2018, pp. 1–6.

[20] Z. Waiming, H. Xiaoxuan, X. Wei, and J. Peng, "A two-phase genetic annealing method for integrated earth observation satellite scheduling problems," *Soft Comput.*, Oct. 2017. [Online]. Available: https://doi.org/10.1007/s00500-017-2889-8

[21] D.-H. Cho, J.-H. Kim, H.-L. Choi, and J. Ahn, "Opitimization-based scheduling method for agile earth-observing satellite constellaation," *J. Aerosp. Inform. Syst.*, vol. 15, no. 11, pp. 611–626, 2018.

[22] Y. Wang, M. Sheng, W. Zhuang, S. Zhang, N. Zhang, R. Liu, and J. Li, "Multi-resource coordinate scheduling for earth observation in space information networks," *IEEE J. Sel. Areas Commun.*, vol. 36, no. 2, pp. 268–279, Feb. 2018.

[23] X. Hu, W. Zhu, B. An, P. Jin, and W. Xia, "A branch and price algorithm for EOS constellation imaging and downloading integrated scheduling problem," *Comput. Oper. Res.*, vol. 104, pp. 74–89, Apr. 2019.

[24] Y. Xiao, S. Zhang, P. Yang, M. You, and J. Huang, "A two-stage flow-shop scheme for the multi-satelllite observation and data downlink scheduling problem considering weather uncertainties," *Rel. Eng. Syst. Saf.*, vol. 188, pp. 263–275, 2019.

[25] M. Lemaitre, G. Verfaillie, F. Jouhaud, J. M. Lachiver, and N. Bataille, "Selecting and scheduling observations of agile satellites," *Aerosp. Sci. Technol.*, vol. 6, no. 5, pp. 367–381, Jul. 2002.

[26] P. Wang, G. Reinelt, P. Gao, and Y. Tan, "A model, a heuristic and a decision support system to solve the scheduling problem of an earth observing satellite constellation," *Comput. Ind. Eng.*, vol. 61, no. 2, pp. 322–335, Feb. 2011.

[27] Q. Dong and W. Dargie, "A survey on mobility and mobility-aware mac protocols in wireless sensor networks," *IEEE Commun. Surv. Tuts.*, vol. 15, no. 1, pp. 88–100, Feb. 2013.

[28] A. Vazintari and P. G. Cottis, "Mobility management in energy constrained self-organizing delay tolerant networks: An autonomic scheme based on game theory," *IEEE Trans. Mobile Comput.*, vol. 15, no. 6, pp. 1401–1411, Jun. 2016.

[29] A. Chakrabarti, A. Sabharwal, and B. Aazhang, "Using predictable observer mobility for power efficient design of sensor networks," in *Proc. IPSN*, 2003.

[30] A. Kansal, M. Rahimi, D. Estrin, W. J. Kaiser, G. J. Pottie, and M. B. Srivastava, "Controlled mobility for sustainable wireless sensor networks," in *Proc. IEEE SECON*, 2004.

[31] V. P. Mhatre, C. Rosenberg, D. Kofman, R. Mazumdar, and N. Shroff, "A minimum cost heterogeneous sensor network with a lifetime constraint," *IEEE Trans. Mobile Comput.*, vol. 4, no. 1, pp. 4–15, Jan. 2005.

[32] F. Marinelli, F. Rossi, S. Nocella, and S. Smriglio, "A lagrangian heuristic for satellite range scheduling with resource constraints," *Comput. Oper. Res.*, vol. 38, no. 11, pp. 1572–1583, Nov. 2011.

[33] W. C. Lin, D. Y. Liao, C. Y. Liu, and Y. Y. Lee, "Daily imaging scheduling of an earth observation satellite," *IEEE Trans. Syst., Man, Cybern. A, Syst., Humans*, vol. 35, no. 2, pp. 213–223, Mar. 2005.

[34] Z. Q. Luo, W. K. Ma, A. M. C. So, Y. Ye, and S. Zhang, "Semidefinite relaxation of quadratic optimization problems," *IEEE Signal Process. Mag.*, vol. 27, no. 3, pp. 20–34, May 2010.

[35] Z. Q. Luo and T. H. Chang, "SDP relaxation of homogeneous quadratic optimization: Approximation bounds and applications," *Convex Optim. Signal Process. Commun.*, pp. 117–165, 2010.

[36] P. Bhardwaj, A. Panwar, O. Ozdemir, E. Masazade, I. Kasperovich, A. L. Drozd, C. K. Mohan, and P. K. Varshney, "Enhanced dynamic spectrum access in multiband cognitive radio networks via optimized resource allocation," *IEEE Trans. Wireless Commun.*, vol. 15, no. 12, pp. 8093–8106, Dec. 2016.

[37] P. A. Diaz-Gomez and D. F. Hougen, "Initial population for genetic algorithms: A metric approach," in *Proc. Int. Conf. Genetic Evol. Methods*, Las Vegas, NV, USA, 2007, pp. 43–49.

[38] G. Hao, P. Li, Q. Dishan, and H. Chuan, "Improved method of acquiring the attitude changing duration of an agile imaging satellite," in *Proc. ICMIC*, Jun. 2012, pp. 24–26.

[39] B. Dilkina and B. Havens, "Agile satellite scheduling via permutation search with constraint propagation," 2005. [Online]. Available: http://www.cs.sfu.ca

Lijun He received the B.S. degree in electronic information science and technology from Anqing Normal University, Anhui, China, in 2013, and the Ph.D. degree in military communications from the State Key Laboratory of ISN, Xidian University, Xi'an, China, in 2020. From September 2018 to September 2019, he was with the University of Toronto, Toronto, ON, Canada, as a Visiting Scholar funded by the China Scholarship Council (CSC). His current research interests include routing, scheduling, resource allocation, and satellite communications.

Ben Liang (S'94-M'01-SM'06-F'18) received honors-simultaneous B.Sc. (valedictorian) and M.Sc. degrees in Electrical Engineering from Polytechnic University (now the engineering school of New York University) in 1997 and the Ph.D. degree in Electrical Engineering with a minor in Computer Science from Cornell University in 2001. He was a visiting lecturer and post-doctoral research associate at Cornell University in the 2001 - 2002 academic year. He joined the Department of Electrical and Computer Engineering at the University of Toronto in 2002, where he is now Professor and L. Lau Chair in Electrical and Computer Engineering. His current research interests are in networked systems and mobile communications. He is an associate editor for the IEEE Transactions on Mobile Computing and has served on the editorial boards of the IEEE Transactions on Communications, the IEEE Transactions on Wireless Communications, and the Wiley Security and Communication Networks. He regularly serves on the organizational and technical committees of a number of conferences. He is a Fellow of IEEE and a member of ACM and Tau Beta Pi.

Jiandong Li (M'96-SM'05-F'21) received the B.E., M.S. and Ph.D. degrees in Communications Engineering from Xidian University, Xi'an, China, in 1982, 1985 and 1991 respectively. He has been a faculty member of the school of Telecommunications Engineering at Xidian University since 1985, where he is currently a professor and vice director of the academic committee of State Key Laboratory of Integrated Service Networks. Prof. Li is a Fellow of IEEE. He was a visiting professor to the Department of Electrical and Computer Engineering at Cornell University from 2002-2003. He served as the General Vice Chair for ChinaCom 2009 and TPC Chair of IEEE ICCC 2013. He was awarded as Distinguished Young Researcher from NSFC and Changjiang Scholar from Ministry of Education, China, respectively. His major research interests include wireless communication theory, cognitive radio and signal processing.

Min Sheng (M'03, SM'16) received the M.Eng and Ph.D. degrees in Communication and Information Systems from Xidian University, Shaanxi, China, in 2000 and 2004, respectively. She is currently a Full Professor at the Broadband Wireless Communications Laboratory, the School of Telecommunication Engineering, Xidian University. Her general research interests include mobile ad hoc networks, wireless sensor networks, wireless mesh networks, third generation (3G)/4th generation (4G) mobile communication systems, dynamic radio resource management (RRM) for integrated services, cross-layer algorithm design and performance evaluation, cognitive radio and networks, cooperative communications, and medium access control (MAC) protocols.